An Experimental Investigation into the Flow Properties of Pharmaceutical and Detergent Powders

A Dissertation submitted
in partial fulfilment of the requirements
for the award of degree of

Master of Engineering

in

Thermal Engineering

by

Vivek Garg

Registration No.: 801583029

Under the Supervision of

DR. S.S. MALLICK

(Associate Professor)

DEPARTMENT OF MECHANICAL ENGINEERING

THAPAR UNIVERSITY, PATIALA

June, 2017

Dedicated to

My Parents and
Maaji

CERTIFICATE

I hereby declare that the thesis entitled "An Experimental Investigation into the Flow Properties of Pharmaceutical and Detergent Powders" is an authentic record of my work carried out as requirements for the award of the degree of Master of Engineering in Thermal Engineering at Thapar University, Patiala, Punjab under the supervision of Dr. S.S. Mallick, Associate Professor, Mechanical Department, Thapar University, Patiala during July, 2015 to June, 2017. No part of the matter embodied in this report has been submitted to any other university or institute for the award of any degree.

Date: 24/05/2017

Vivek Garg

It is certified that the above statement made by the student is correct to the best of my/our knowledge and belief.

25/5/17

Dr. S.S. Mallick
Mechanical Engineering Department
Thapar University, Patiala – 147004

i

Acknowledgement

I would like to acknowledge my supervisor Dr. S.S. Mallick for introducing me to the fundamentals of research. He provided an excellent atmosphere necessary for a research scholar to carry out his research work. His advice and pointers were priceless and had a deep impact on my analytical thinking and research work as well.

Vivek Garg

Abstract

This thesis presents results of an investigation into the flow properties of six popular pharmaceutical powders (Active Pharmaceutical Ingredient: Lactose and Paracetamol, Excipients: Calcium Sulphate, Di-Calcium Phosphate, Magnesium Tri-Silicate and Starch) and one sample of detergent powder and the effects of the same on designing storage facilities with and without considering the influence of time consolidation. Several processing industries face challenges of no flow (arching), inadequate flows, improper powder compaction, segregation etc. due to the lack of fundamental understanding of powder flow properties and their effects on selection of hopper half-angles and outlet sizing. Physical properties such as particle size, specific surface area, porosity, density was investigated. Flow properties (both instantaneous and time consolidation) of all the powder samples were tested on Powder Flow Tester (ring shear tester), manufactured by Brookfield, USA. It was observed, after the time consolidation test, Paracetamol changed its flow characteristics from “cohesive” to “very cohesive”, Lactose from “easy flowing” to “very cohesive”, Starch from “easy flowing” to “cohesive”, Detergent from “free flowing” to “cohesive” whereas other powders (Calcium Sulphate, Di-Calcium Phosphate, Magnesium Tri-Silicate) did not change their flowability characteristics. Using the flow function and the wall friction data, hopper half angle and hopper outlet dimensions were estimated. The results showed that the powders such as Paracetamol, Detergent, Calcium Sulphate and Magnesium Tri-Silicate requires wider hopper outlet dimension. For a good design, the engineer is recommended to carry out necessary flow property testing with and without time consolidation effects into consideration for designing practical storage or feeding systems to achieve desirable mass flow condition.

Keywords: flow property testing; pharmaceutical powders; detergent; flow function; time consolidation; hopper design.

Contents

List of Figures

List of Tables

Nomenclature

C	Cohesion, kPa
D	Minimum opening size, mm
mg	Particle weight, N
d	Particle size diameter, μm

Greek Symbols

θ	Hopper half angle, °
σ	consolidation stress or normal stress, kPa
σ_{pre}	Pre shear stress, kPa
τ	Shear stress, kPa
σ_1	Major principle stress, kPa
σ_c	Unconfined yield strength, kPa
φ	Angle of internal friction, °
ρ_{lb}	Loose poured bulk density, Kg/m^3
ρ_p	Particle density, Kg/m^3
ρ_t	Tapped bulk density, Kg/m^3
φ_w	Wall friction angle, °
$\sigma_{c,\ min}$	Minimum unconfined yield strength, kPa

δ	Effective angle of internal friction, in degrees

Acronyms

FI	Flow Index
RH	Relative Humidity
PFT	Powder Flow Tester
SEM	Scanning Electron Microscopy
SSA	Specific Surface Area

Chapter-1

Introduction and Objectives

1.1 Introduction

In pharmaceutical industries, the active pharmaceutical ingredients and excipients combine together to form the final drug after passing through various processes, such as blending, transfer, storage, feeding, die filling, fluidization and encapsulation. There are various challenges being faced by pharmaceutical industries due to improper flowability of powders (Ripp. et al., 2015). During the different processes through which the powders pass through in the pharmaceutical industry, the powders undergo significant variation in their physical properties, such as in powder flowability, bulk density etc. Therefore, to maintain the efficiency of these processes, it is vital to monitor these variations. Apart from this, there could be a possibility of powder agglomeration, which would result in blockage, unstable discharge and subsequent stoppage of the equipment and processes. On the other side, excessive free flowing of powders would cause more flooding of the pharmaceutical powders during filling operation, thus again compromising on the process and product quality. Therefore, it is mandatory to monitor the flowability variation at each unit with close precision (Koynov et al.,2015) and take appropriate measures to ensure that the desirable powder flowability is maintained. To investigate into the flowability of different powders through various equipment's, the standard procedure is to perform laboratory scale test based on Jenike's principle (Schulze, 2008). The method comprises of calculating flow function coefficient and generating flow function curves under instantaneous and time consolidation stresses (Ripp. et al.,

2015). Other parameters, such as unconfined yield strength, cohesion and angle of internal friction, can be calculated by analyzing the Mohr's circle with the knowledge of major principal or consolidated stresses (Bian et al.,2015). There are various powder characteristics, such as particle size distribution, particle shape, surface structure, particle density, bulk density, water content and chemical composition on which flowability of powder depends. To characterize the flow properties of the powders, shear cell technique is widely used (Amagliani et al., 2016) in designing storage bins and hoppers that are widely used in industries, such as detergent, cement, food etc. (Fitzpatrick et al., 2004). However, it seems that there is a limited amount of information available in open literature on the flowability of powders used in pharmaceutical industries. The nature of most of the pharmaceutical drugs are solid crystalline and the processes in which they go through are quite delicate to parameter variation, which may alter the medicinal value of the powder, making them either ineffective or dangerous to human health. To maintain the desired quality control on the drugs, it is essential to pre-determine the powder flowability and to investigate whether the powder contains the right mixture of all the required ingredients. Requisite amount of powder flowability should be maintained for high speed tableting and encapsulation processes (Dudhat et al., 2016). Use of glidants have become quite common for most of the pharmaceutical industries in order to reduce the issues of powder agglomeration and to maintain the powder flowability (Trementozzi et al., 2017). However, it has been reported that excess use of glidants may disturb the surface morphology and decrease the solubility time of the drugs affecting the hardness range of the tablets (Morin and Briens, 2013). Hence, to maintain better flowability of the powders without the use of glidants, it is essential to design the storage facilities correctly with a thorough knowledge of the powder flowability. Hence, there is a need to carry out research on the flowability of pharmaceutical powders. Similarly, it seems that there is a limited amount of information available

in open literature on the flowability of detergent powders. The nature of most of the detergents are solid amorphous and the processes in which they go through are quite delicate to parameter variation, which may alter the chemicals of the powder, making them ineffective. To maintain the desired quality control, it is essential to pre-determine the powder flowability and to investigate whether the powder contains the right mixture of all the required chemicals. Requisite amount of powder flowability should be maintained for high speed tableting and encapsulation processes (Dudhat et al., 2016). Use of binders have become quite common for most of the detergent manufacturing industries in order to reduce the issues of powder agglomeration and to maintain the powder flowability (Trementozzi et al., 2017). However, it has been reported that excess use of binders may disturb the surface morphology and decrease the solubility time of the detergent powder affecting the hardness range of the detergent tablet (Morin and Briens, 2013). Hence, to maintain better flowability of the powders without the use of binders, it is essential to design the storage facilities correctly with a thorough knowledge of the powder flowability. Hence, there is a need to carry out research on the flowability of detergent powders.

Powder flowability characteristics can get significantly changed due to inventory, e.g. long storage period could result in compacted bulk powders, which would subsequently reduce the powder flowability due to the gain in strength. This could be caused by a possible change in the physio-chemical interaction within the particles and the surrounding ambience of the storage place (temperature, relative humidity etc., Sun, 2016)). Limited amount of literature is available which demonstrates the comparison between instantaneous and time consolidation flow characteristics (Wang et al., 2016). Studies on the time consolidation effect on the powder behavior have been carried out mainly for the food powders (Slettengren et al, 2016), but such information is generally

missing for the pharmaceutical powders (as reported by Wang et al., 2016). Therefore, it is needed to carry out an investigation on the pharmaceutical powders with and without the effect of time consolidation for better designing of storage facilities. The aim of this thesis is to investigate into the flow properties of various pharmaceutical and detergent powders subjected to instantaneous and time consolidation conditions and to use such information to effectively design industrial storage systems. The aim is to provide the industry a reliable design guidelines to enable the powders to flow adequately under the influence of gravity, without the requirement of artificially improving the flowability of the powders that may compromise with the medicinal effectiveness of the drugs. The literature reports (Jan et al., 2016) that during consolidation and under the influence of inter-particle adhesive forces, cohesive arches are formed. Usually, two types of flow patterns of powders are prevalent in storage hoppers: mass and funnel flow. The more desirable mode is the mass flow, because in this type of flow, all the particles flow simultaneously on first-in, first out basis, thus assisting in achieving better product and process quality control. Powders such as lactose and paracetamol (Pharmaceutical API's), calcium sulphate, di-calcium phosphate, starch, magnesium tri-silicate (Pharmaceutical Excipients), are widely used in pharmaceutical industries and hence, these have been studied in this thesis. Additionally, similar studies have been investigated on the detergent powder due to its wide range of application in industries.

1.2 Objectives

(1) To perform physical characterization on six different pharmaceutical powders (Lactose, Paracetamol, Calcium Sulphate, Di-Calcium Phosphate, Magnesium Tri-Silicate and Starch) and Detergent powder.

(2) To investigate into the flow properties (flow function, angle of internal friction etc.) of the above powders under instantaneous and time consolidation effect using a ring shear tester.

(3) To investigate into the wall friction characteristics of the above powders.

(4) To design and evaluate hopper half angle and the hopper outlet dimension under instantaneous and time consolidation loading conditions.

Chapter-2

Literature Review

This chapter is divided into two parts. The first part comprises of the introduction of bulk storage facilities and problems caused by improper flow due to the lack of fundamental understanding of powder flow properties., second part consist of comprehensive literature review of different previous research work.

2.1 Common problems with bulk solids flow in storage facilities

Arching is the most common problem encountered in industrial bulk solids storage facilities and is caused by the cohesive strength of fine powders and due to interlocking in coarse particles. Funnel flow and rat holing are also the major problems faced during the discharge of bulk solids from the silos/hoppers. The funnel flow mainly occurs due to large hopper half angle and high wall friction. Due to large hopper angles, the material remains stagnant with the walls and over the time gains the strength. Further, the residence time is another major point of concern in the funnel flow silo. The material which is filled recently comes out of the silo without complete de-aeration and the fine powders flow similar to fluid flooding from the outlet of the silo. Hoppers with screw feeders face the problem non-uniform discharge. The material at the extreme left/right of the hopper is actively discharged while rest of the feeder do not give any discharge. Segregation occurs in the silo when it is centrally charged. The fines accumulate at the centre of the silo, while the

coarse particle roll down the walls of the silo and during discharge, the fine particles comes out of the hopper first and followed by the coarse particles. Segregation is the major problem in chemical and pharmaceutical industries as different types of powders have different size/shape and they segregate during various handling operation. Eccentric discharge in the silo is caused due to unsymmetrical loading over the silo during discharge of the silo. This causes buckling in the silo and further changes the flow pattern in the silo. The design procedure developed by Jenike is the cornerstone in the designing of the silo and hoppers. This procedure is adopted commercially for the designing of the industrial grade silos. The major part of the of the design procedure includes: estimation of opening size for the silo and the hopper half angle.

2.2 Review of the previous research on powder flowability

Geldart et al (1999) confirmed that the increase of particle size of a powder mixture is always accompanied by the decrease in cohesivity. When powder mixtures are dominated by fine particles, the interparticle forces, in this case the van der Waals forces, should be dominant in the packing of particles. Due to this, low aerated densities are registered when the particle size is small. The increase in particle size slowly diminishes the influence of the van der Waals force, thus causing the aerated density to increase. The increase in mean particle size has a great influence on the arrangement of particles as they try to form the densest packing. It should be remembered that a large mean particle size corresponds to a small percentage of the fine components. In a segregating system, when powder is given mobility by tapping, the large and small particles are able to rearrange to form the densest packing. More large particles will provide more unoccupied

voids as most of the small particles would migrate to the bottom of the cup to fill those voids in the lower region. Therefore, the reason for the lower tapped density observed for mixtures with smaller percentage of fine particles is simply that there are not enough fine particles to fill the voids in between the large particles. It is believed that the fine particles in these mixtures coated the larger particles, and the repeated tapping simply could not dislodge the fine particles from the larger particles. The primary structure remains and there is no increase in tapped density as no rearrangement of particles occurs. Hausner ratio increases with the decrease of particle size.

Teunou et al. (1999) investigated on the flow properties of food powders. They did experimentation on the annular shear tester to measure the powders flowability. Various physical properties such as particle density, loose poured bulk density, water sorption isotherms were investigated to define the characteristics of the powders. Effect of temperature and relative humidity was studied by generating instantaneous flow function curves. Design of hopper was predicted after determination of flow parameters. It was observed, Tea powder showed hygroscopic characteristics in nature and it has smaller particle size. It was concluded that tea powder does not flow properly at high relative humidity. The effect of relative humidity on the flour was not much observed because it is already cohesive in nature. Other products were not flowing better at high relative humidity because of their caking property.

Fitzpatrick et al. (2004) characterized the flow properties of thirteen different kinds of food powders. Particle size ranged from 12- 320 μm. The maximum particle density was 2200 kg/m^3 and the minimum was 1490 kg/m^3. The range of effective angle of internal friction varied from 40° to 65°. It was investigated that there was no relation of physical properties with the flowability

characteristics of the powder. To design the dimension of the hopper, the authors used the basic principle approach i.e. Jenike's approach. Using Jenike's methodology, one can determine the hopper half angle and minimum opening size for the hopper. The authors emphasized on the importance of Jenike's method for hopper design by showing the sensitiveness of the method. It was investigated, this methodology gave low values of unconfined yield strength and outlet opening size.

Iqbal et al. (2004) emphasized on the characteristics of powder flowability by observing the effect of different storage condition such as relative humidity, temperature etc. on the flowability of three food powders. The food powder includes; flour (73μm), tea powder (25μm), and whey-permeate (98μm). There were many changes observed after storing these powders for seven days. Some powders became cohesive due to their hygroscopic characteristics, while powders like flour remain unchanged because they all cohesive itself. This study investigated the effect of temperature on the flowability, hence, affecting the design of the hopper/silo.

Tang et al. (2004) reviewed various methods to minimize segregation in silos. They advocated that four different mechanisms are responsible for the segregation, which are trajectory, sieving, fluidization, agglomeration. Improvement in material properties, such as narrowing down of the particle size distribution and avoiding irregular shaped particles help in reduction of segregation. Proper selection of material handling equipment and operational parameters, such as lowering of the free fall distance and using mass flow silos reduces segregation. Second generation primary shear cell was developed by the authors to study the sieving and percolation mechanism of segregation.

Ganesan et al. (2008) investigated the effect of various parameters such as pressure, temperature etc. on the powder flow properties. The material for the experimentation was Distilleries Dried grains with soluble (DDGS). It is obtained when ethanol is extracted from the maize. It has a wide range of application, especially, it is used as a source of protein. Different flow properties such as angle of internal friction, frictional properties were determined using different types of methodology such as ring shear tester, direct shear tester and Carr's index. The comparison in the flow behaviour was then made and it was observed that shear cell tester gave better results for the flowability of the powders.

Schulze (2008) reported that the quantitative relationship between the two parameters remains to be identified, the qualitative resemblance is not surprising. The parameters f_c and τ_c describe the powder strength and the cohesion, respectively. It is not surprising that a more cohesive powder has a higher strength. Higher cohesion is associated with less efficient packing of the powder (e.g., easier formation of air pockets), which contributes to the further decrease in powder ρb. This is expected if the steeper decrease in ρb with Relative Humidity (RH) indeed includes the contribution from less efficient packing of particles because air pockets are broken under stress so that impact of packing efficiency on powder density is reduced.

Emery et al. (2009) studied the effect of moisture on the flowability of pharmaceutical powders. The author tried to investigate which flowability test gives more accurate results for determining the effect of moisture. The author used four powders with each powder having different percentage of moisture content. Different Flowability tests were Hausner Ratio test, Carr Index test, Angle of

repose test, Jenike's Shear test. The author used MATLAB (Least Square Technique) for shear cell tester. The author concluded that though Jenike's Shear test takes time, but it is the most accurate method for determining the effect of moisture on different types of powders.

Geldart et al. (2009) investigated the effect of Angle of repose on the flowability of the powder. Three standard flowability measuring equipment naming Johnson indicizer cohesion tester, warren Bradford spring cohesion tester, Jenike shear tester results were used to find the correlation between flowability of powder and AOR. It was observed that as the fine Particles increases, the repose angle also increased. The material taken for the experimentation was the mixture of two powder BACO FRF (flame retardant filters) having chemical formula $Al_2O_3.3H_2O$ of different particle size. Different particle size was taken so that blend can be composed properly. The authors developed their own tester which qualitatively measure the powder flowability based on angle of repose.

Lumay et al. (2012) measured the flow properties of silicon carbide, flour and rice. They investigated that granular material is a system which is complex and in which the transitions of states takes place, which are: static state followed by a quasi-static state and finally the dynamic state. The author inspected that by investigating the heap's height and the angle of repose, one can achieve the steady state. The quasi state can be measured by conducting Hausner Ratio (HR) tests. It was observed that, the powder may have same Hausner Ratio but their dynamics of getting compacted can be different. Different plotting trends were shown by the author in relation to void fraction and tapped density. It was also investigated that the property such as cohesiveness plays

a vital role in determining the angle of repose. Flow properties of the material was measured at different consolidating stresses.

Leturia et al. (2014) investigated and contributed in comparing different methods which are used to measure the characteristics of the powder. The investigation was carried on seven different powders. The testing which was used long years back were categorised into three parts i.e. testing under aerated, free surface and packed bed conditions. One can classify the material on the basis of the stress which material can bear. It was investigated that only one index is not enough to predict or classify the flow characteristics of the powder. The author found, for defining the flow property of the material one has to perform various testing techniques to get the complete understanding of the behaviour of the powder and also to study the impact of different storage condition on the powder.

Marrup et al. (2014) investigated and developed a new simple mono-axial shear tester which determine the flowability of cement. Tests were performed at three different consolidation stresses i.e. 0.94, 1.87, 2.79 kPa. It was observed that the flow function curve was almost constant up to 550°C, but above this temperature, large deviations were found, hence change in the flow behaviour of the powder. The flowability of powder reduced above 550°C due to Calcination and Bellite formation. It was observed that, the material has a tendency to flow better when unheated. The observation was made on the basis of the results which mono-axial shear tester gave. It was also investigated that the chemical composition of the material also plays an important role in the flowability of the powder.

Amagliani et al. (2016) investigated that the flowability generally decreases with decreasing particle size, as there is more contact area between particles for cohesive and frictional forces which resist flowability. The flowability of powder are influenced by shape and surface characteristics. Lactose powders with a more spherical shape have been reported to have higher flowability and lower compressibility; the more spherical shape is thought to reduce particle interlocking and resistance to flow. Also, surface roughness can promote interactions between particles by Van der Waals forces and mechanical interlocking, and thus increase cohesiveness. Flow properties of the powders was also influenced by the major principal consolidating stress (MPCS) applied, which means that powders would be expected to have different flow behaviour in different regions of a hopper (i.e., the converging section of a silo) and at different fill heights therein. Flowability of food powders is impaired due to the presence of surface fat as it allows the particles to agglomerate through liquid bridging. The high fat content suggests that the particle surface might be covered with fat to some extent, which would impair its flowability. As previously outlined, flowability tends to decrease with a reduction in particle size; The results suggest that chemical composition, particle shape and surface characteristics impacted the flowability of the powders more strongly than the particle size. It was also investigated that the minimum hopper angle required to ensure mass flow depends on the friction between the hopper wall material and the powder.

Li et al (2016) reported that circularity, convexity and elongation are three commonly used shape factors. One way to measure shape is to quantify how close the shape is to a perfect circle. A perfect circle has a circularity of 1 while a ‘spiky’ or irregular object has a circularity value closer to 0. Circularity is sensitive to both overall form and surface roughness. Elongation is defined as

[1-aspect ratio] or [1-width/length]. A shape symmetrical in all axes, such as a circle or square, has an elongation value of 0; shapes with large aspect ratios have an elongation closer to 1. Convexity is a measurement of the surface roughness of a particle. It is calculated by dividing the convex hull perimeter by the actual particle perimeter. A smooth shape has a convexity of 1 while a very 'spiky' or irregular object has a convexity closer to 0. Furthermore, morphological study showed that dairy solids with lower crystallinity had more rounded shape, and smoother surface. Wall friction is the dominant parameter in determining the minimum hopper angle (between the hopper wall and the horizontal) required to ensure mass flow.

Roos et al (2016) indicated that particle shape of lactose/MPI solids systems with higher content of lactose had less rounded shape, rougher surface and lower ratio of width/length. Moreover, the more the particles in a powder resemble spheres the better the powder flows. Coarse powders in general have better flow properties than fine powders. Consequently, the difference in particle shape of lactose/MPI solids systems might influence the final flow properties of spray-dried dairy solids. The wall friction angle, quantifies the effort required to move a bulk solid across the surface of a specific wall material. The larger the wall friction angle, the greater is wall friction, which can result in deposition or segregation of powder.. Powders with smaller particle sizes tend to increase wall friction, as there is greater contact surface area between smaller particles and the wall surface. They also exhibited less rounded, rougher surface and higher ratio of length to width shapes based on the significantly lower values of circularity, convexity and higher values of elongation .It is commonly believed that the granules without consolidation will grow progressively by layering materials on the surface, while consolidation supplied by strong mechanical agitation will lead to

plastic deformation of granules via a process of squeezing-out entrapped air, increased internal pore saturation and reduced porosity.

Ji et al (2017) investigated that adhesive forces are usually the source of such flow problems for fine-grained dry bulk solids. The major adhesive forces are based on van der Waals interactions and the intensity of the forces mainly depend on the particle size as well as the distances between individual particles. When the distances are small or the surfaces of particles are in contact, van der Waals forces have a large influence. Therefore, plastic deformation and rearrangement occurring at contact points may cause an increase in adhesive forces. In addition, smooth and spherical particles usually flow better than rough and non-spherical particles. It is clear that decreasing particle size resulted in increased wall friction angles, regardless of the normal stresses applied. There is a greater tendency for the granules with high wall friction angles to undergo deposition or segregation in a hopper, as the particles near the hopper walls move slower than that in the centre. Thus, high wall friction may lead to the materials near the walls discharging finally

Chapter-3

Materials and Methods

3.1 Characterization of powders

In the present study, samples of calcium sulphate and di-calcium phosphate powders were obtained from VIP Pharmaceuticals Pvt. Ltd. Each sample was preheated in a baking oven at 103°C for 3 hours for the purpose of removing any moisture content as per ASTM D 2974-87. Chemical characterization of the samples was tested using Energy-dispersive X-ray spectroscopy. In lactose powder sample, it was found that carbon contains 49.92% by weight, whereas oxygen contains 50.08% by weight. In Paracetamol powder sample, the weight percentage of carbon, nitrogen and oxygen were 52.40, 22.24 and 25.36, respectively. In Di-Calcium Phosphate powder sample, the weight percentage of calcium, phosphate and oxygen were 41.29, 12.72 and 45.99%, respectively. In Calcium Sulphate powder sample, calcium, Sulphur and oxygen contents were 19.35, 17.44 and 63.21% by weight, respectively. In Starch powder sample, it was found that carbon content is 53.60% by weight, whereas oxygen content is 46.40% by weight. In Magnesium Tri-Silicate powder sample, the weight percentage of Magnesium, Silicon and oxygen were 11.45, 17.41 and 71.14, respectively. The results of chemical composition of Detergent are illustrated in Table 1

Table 3.1: Chemical composition of the detergent powder

Element	**% by weight**
Carbon	19.25
Sodium	11.41
Magnesium	0.14
Aluminium	0.13
Sulphur	0.13
Chlorine	13.11
Calcium	0.11
Oxygen	55.71

Particle size distribution and specific surface area

Particle size distribution and specific surface area (SSA) of the powders were determined by laser light scattering using a Malvern Mastersizer 3000 (Malvern Instruments, Worcestershire, UK) instrument. Span values were determined using equation 3.1.1 to evaluate the particle size distribution.

$$\text{Span} = (d_{90}-d_{10})/d_{50} \qquad (3.1.1)$$

where, d_{50} represents the diameter below which half of the powder population lies. 10 and 90% of the distribution lies below the size values of d_{10} and d_{90}, respectively.

Bulk and particle densities

The bulk density of a powder is defined as the mass of powder divided by the volume occupied. The bulk density of a powder can undergo considerable changes depending on the different processes through which the bulk powder passes, such as packing, compaction, consolidation, fluidization etc. Loose poured bulk density represents the random loose packing of a powder and its value is measured by allowing mildly aerated powders to get settled in a container under the influence of gravity (without the application of any other external loading). A powder with a strong structural strength (i.e. strong particle-particle-wall bonding) will exhibit a low bulk density, as it will tend to resist collapsing when dispersed in a container. Furthermore, high friction between the particles will resist rearrangement of the powders towards achieving high packing density, thus contributing to low bulk density. On the other side, a structurally weak powder will exhibit a high bulk density, as it will collapse readily when left to settle, especially under tapping. Also, low friction between the particles will facilitate in easier realignment of particles, which in turn would result in stronger packing and bulk density (Abdullah and Geldart, 1999). Porosity (Li et al., 2016) and compressibility index (Ji et al., 2017) were determined using the following formulae:

$$\text{Porosity} = 1 - (\rho_{lb}/\rho_p) \qquad (3.1.2)$$

Compressibility Index = $100 \times [1- (\rho_{lb} / \rho_t)]$ (3.1.3)

Particle density (ρ_p) of samples was determined using water displacement method. The ratio of the tapped to loose poured bulk density is defined as the Hausner ratio, which is a known as useful measure of cohesion and particle to particle friction (Abdullah and Geldart, 1999). A drop in the value of Hausner ratio represents decrease in cohesiveness of the powders.

Scanning Electron Microscopy

Scanning Electron Microscope (SEM) images were captured at the Sophisticated Analytical Instruments Laboratory of Thapar University, Patiala. The powders were placed on Aluminium stubs using double-sided carbon tape and coated with a 5-mm layer of gold/palladium (Au: Pd ¼ 80:20) in JSM-5510 Scanning Electron Microscope (make: JEOL Ltd), The instrument was operated at an accelerating voltage of 15 kV and the images were taken at a magnification of 1000.

3.2 Powder flow property testing

Powder Flow Tester (PFT) of Brookfield Engineering Laboratories, Inc., Middleboro, MA, USA was used to experimentally determine the flow properties of calcium sulphate and di-calcium phosphate at the Laboratory for Particle and Bulk Solid Technologies, Thapar University. Powder Flow Tester (PFT) works on Jenike's methodology. It has an annular shear cell, in which the sample is filled and the lid is placed on the top increases the consolidation stress over the powder.

The axial and torsional speeds for the PFT were 1.0 mm/s and 1 rev/hr., respectively. These were applied to produce shear in the sample under a given consolidation stress. Samples were filled into the Aluminium trough of the annular shear cell at room temperature (22 to 25°C). The powder surface in the trough for flow- or wall-fiction tests were levelled using curved- or flat-profiled shaping blades, respectively. Of the two available lids, the flow function lid was used to measure yield locus in the powder and wall friction tests were conducted with standard wall friction lid made of 304 stainless steel with 2B surface finish. Vane or flat profiled lids were attached to compression plate for flow or wall friction tests. The equipment was automated with the Powder Flow Pro software for analysis of the raw data and providing yield locus, flow function curves, trends for wall friction angle versus normal stress, angle of internal friction versus major principle consolidating stress, time consolidation information and hopper half angle. For the standard flow function tests, the applied uniaxial normal stresses were between 0.2 and 4.8 kPa. Ten normal stresses were applied between 0.4 and 4.8 kPa to measure the wall friction angles for the standard wall friction tests. Leung et al. (2016) also has used Powder Flow Tester (PFT) to determine the flow properties of the bulk powders.

Chapter-4

Results and Discussions

In this chapter, the results of physical property testing, flow property testing, hopper design with and without considering the time consolidation effect have been provided. The results are provided as per the chronological order in which the work was performed: the results related to the pharmaceutical powders have been provided in pairs [(Lactose and Paracetamol), (Calcium Sulphate and Di-Calcium Phosphate), (Magnesium Tri-Silicate and Starch)]. The results for the detergent powders are provided in solo.

4.1 Results and discussion for Lactose and Paracetamol

4.1.1 Physical properties of powders

Table 1 lists the various physical properties of lactose and paracetamol. Figure 1 shows the Scanning Electron Microscopy (SEM) images of lactose and paracetamol powders. Chemically, lactose and paracetamol powders are known as β-D-galactopyranosyl-(1→4)-D-glucose and *N-(4-hydroxyphenylacetamide)*, respectively. Table 4.1.1 shows that the average particle size of paracetamol powders is less than that of lactose powders, indicating the presence of more fines in paracetamol powders. As a result, the specific surface area is also more for paracetamol powders (Table 1). Smaller particle size and the prevalence of more fines would result in larger amounts of Van der Waals forces of attraction (adhesion) amongst the particles in case of paracetamol powders

(Sun, 2016). Also, the SEM images provided in Figure 4.1.1 shows that the lactose powders were having relatively more uniform and smooth shapes compared to the paracetamol powders (Li, 2016). Though not exactly spherical, but the lactose powders seem to have less ratio of length to width compared to paracetamol (and hence, closer to having a spherical shape) compared to the paracetamol powders which appears to have several needles like, irregular appearance (having higher length to width ratio). The more the structure is irregular/needle type (away from spherical), the more is the resistance of the powders to flow under disturbance (such as tapping) or under compressive load. This is due to the fact that the spherical or closer to spherical shaped particles with smooth surface (lactose) would move against each other more easily compared to irregular or needle shape particles such as paracetamol, where the particles would experience greater frictional resistance to flow pass each other due to the larger surface roughness. Additionally, larger specific surface area of paracetamol powders would further contribute to surface resistance (Amagliani et al, 2016). It can be seen from Table 4.1.1 that the loose poured bulk density of paracetamol powders is less than lactose powders. This further confirms that the paracetamol powders exhibit greater particle-particle adhesion and as a result, these powders do not settle down easily under gravity by moving against each other and causing relative realignment in position and orientation. On the contrary, the lack of cohesion amongst the lactose powders have resulted into higher bulk density as the particles were relatively freer to move against each other, reorient and occupy interparticle void spaces. For the same reason, it has been found (Table 4.1.1) that the porosity of paracetamol powders is more than lactose. This gets further validated by the values of Hausner ratio (Table 4.1.1). The Hausner ratio value of paracetamol is more than lactose indicating that the paracetamol powders can be compressed to relatively larger tapped density than lactose powders. This suggests that the paracetamol powders have stronger particle-particle cohesion and will

exhibit poor flowability lactose powders. The reason for achieving relatively larger tapped density for paracetamol is that the paracetamol powders were having larger porosity (i.e. larger particle to particle air gaps) in the first place (loose poured condition) (Abdullah et al, 1999). Upon tapping, the paracetamol powders were forced to occupy those void spaces. As the lactose powders were having relatively lesser amount of void spaces in the first place (loose poured condition), hence these powders had only fewer void spaces for the fines to occupy under tapping condition. Therefore, the results of particle size, surface area, bulk density, Hausner ratio and porosity all indicate that the paracetamol powders are likely to be a poorer flowable powder compared to lactose powders. Span was determined using equation 4.1.1 to evaluate the range of size distribution.

$$\text{Span} = (d_{90}-d_{10})/d_{50} \quad (4.1.1)$$

Where, d_{50} is defined as the diameter below which half of the powder population lies. Similarly, 10 and 90% of the distribution lies below the size values of d_{10} and d_{90}, respectively.

Porosity (Li et al, 2016) and compressibility index (Ji et al, 2017) were calculated using the following formulae:

$$\text{Porosity} = 1-(\rho_{lb}/\rho_p) \quad (4.1.2)$$

$$\text{Compressibility Index} = 100 \times [1-(\rho_{lb}/\rho_t)] \quad (4.1.3)$$

Table 4.1.1: Physical properties of lactose and paracetamol

Powders	**d_{10} (µm)**	**d_{50} (µm)**	**d_{90} (µm)**	**ρ_{lb} (kg/m^3)**	**ρ_p (kg/m^3)**	**ρ_t (kg/m^3)**	**HR**	**CI**	**Porosity**	**Span**	**SSA (m^2/kg)**
Lactose	10	64	158	620	1600	787	1.27	21.21	0.61	2.31	157
Paracetamol	6	22	62	482	1700	655	1.36	26.41	0.72	2.54	226

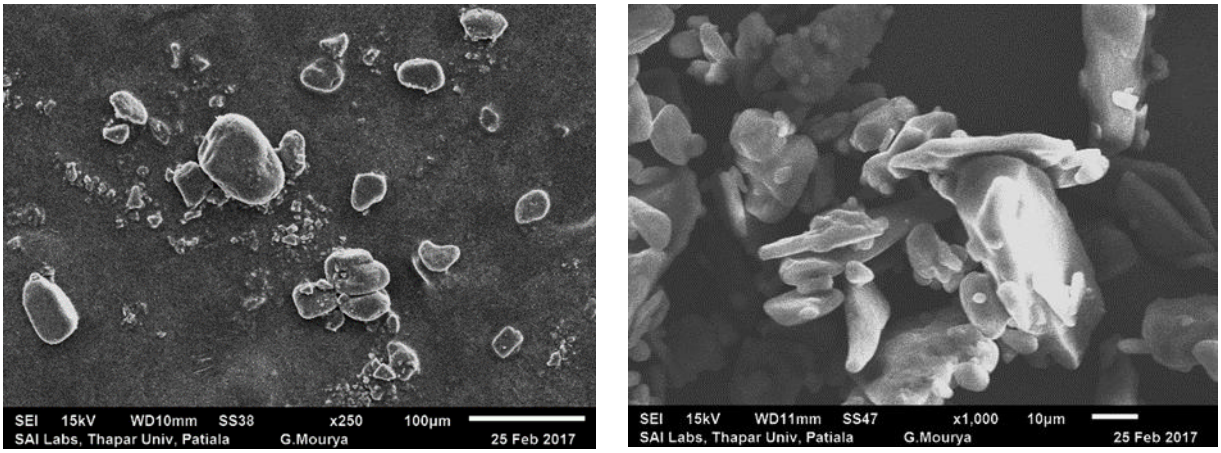

(a) Lactose sample (b) Paracetamol sample

Figure 4.1.1: SEM Images of lactose and paracetamol samples

4.1.2 Flow properties of lactose and paracetamol powders

Yield locus and flow function curves

Yield locus of powder sample signifies the shear stress (τ) necessary to initiate the flow in the powder sample under a given consolidation stress (σ) (Schulze, 2008). Yield locus is a curve which is generated between normal consolidation stress and shear stress. Yield locus at any given pre-shear stress can be represented by Equation 4.1.4.

$$\tau = \sigma \tan \varphi + C \qquad (4.1.4)$$

Where, φ is the angle of internal friction representing the magnitude of friction between the layers of powder. The values of pre-shear stresses for lactose were 0.306, 0.603, 1.201, 2.407 and 4.843

kPa, whereas the same for paracetamol powders were 0.3, 0.596, 1.195, 2.402 and 4.839 kPa, respectively. Each yield locus provides major consolidation stress (σ_1) on the powder sample and unconfined yield strength (σ_c) of the powder. Flow function curve is plotted between σ_1 and σ_c. Figure 2 shows the flow function curves for paracetamol and lactose. The flow function curve has been divided in four parts on the basis of Jenike's flowability classification (Jager et al, 2015), as reported by Saw et al 2015. Flow Index (FI), which is the reciprocal of flow function curve slope (σ_1/σ_c), represents the relative flowability of the samples. Typical values of Flow Index (FI) and the slope of flow function curve for lactose at a pre-shear value of 1.2 kPa were 1.245 and 0.35, respectively. Values of the same parameters under the same pre-shear values for paracetamol were 1.967 and 0.47, respectively. Figure 4.1.2 shows that below a major principal consolidation stress of about 2.5 kPa, the lactose powder fell in the "cohesive" regime. However, above this consolidation stress (2.5 to 10 kPa range), the lactose powder fell into the "easy flow" regime. On the contrary, the paracetamol powders remained in the "cohesive" regime in the entire range of consolidation stress (0 to 10 kPa). The reason for paracetamol being more cohesive compared to lactose powder has been already explained in the previous section. Figure 4.1.2 shows the flow function curves for lactose and paracetamol based on instantaneous flow function results.

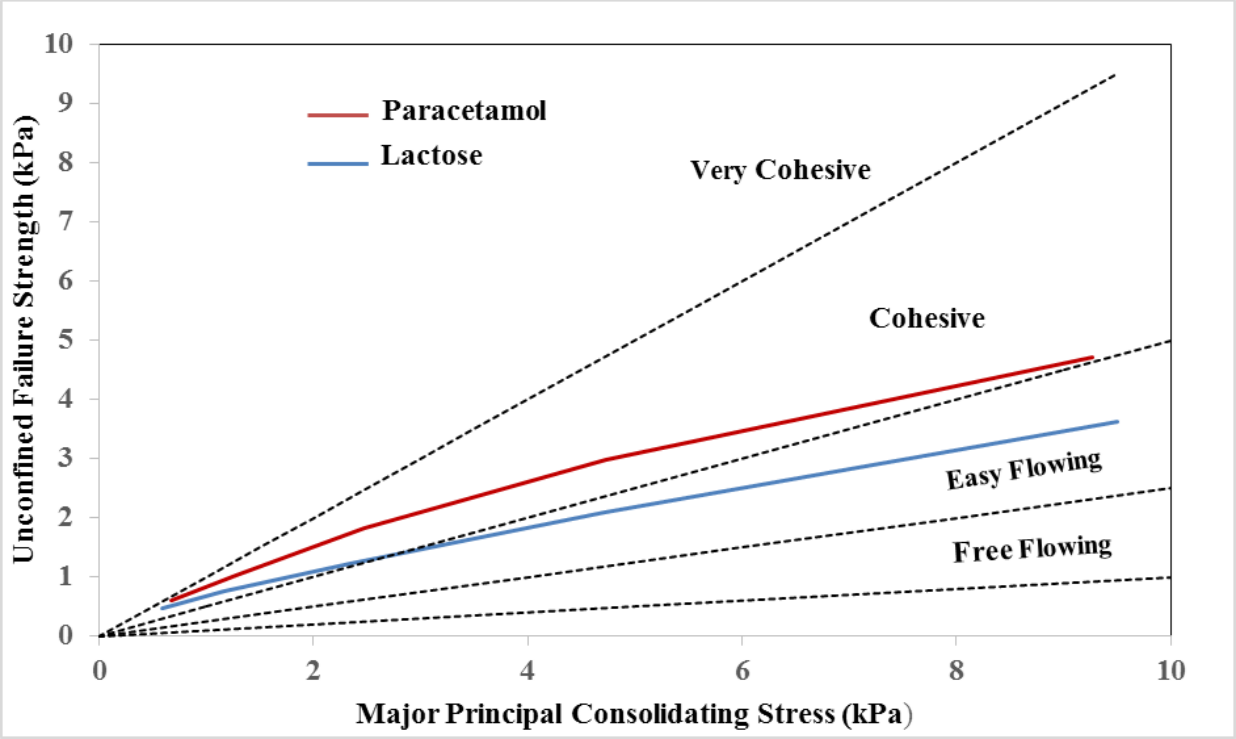

Figure 4.1.2: Flow function curves for paracetamol and lactose powders based on instantaneous flow function test results

Effective angle of internal friction (δ) is the ratio of major consolidation and minor consolidation stresses over the powder element in steady state flow (Jenike,1964). The variation of effective angle of internal friction with major consolidation stress is given in Figure 4.1.3.

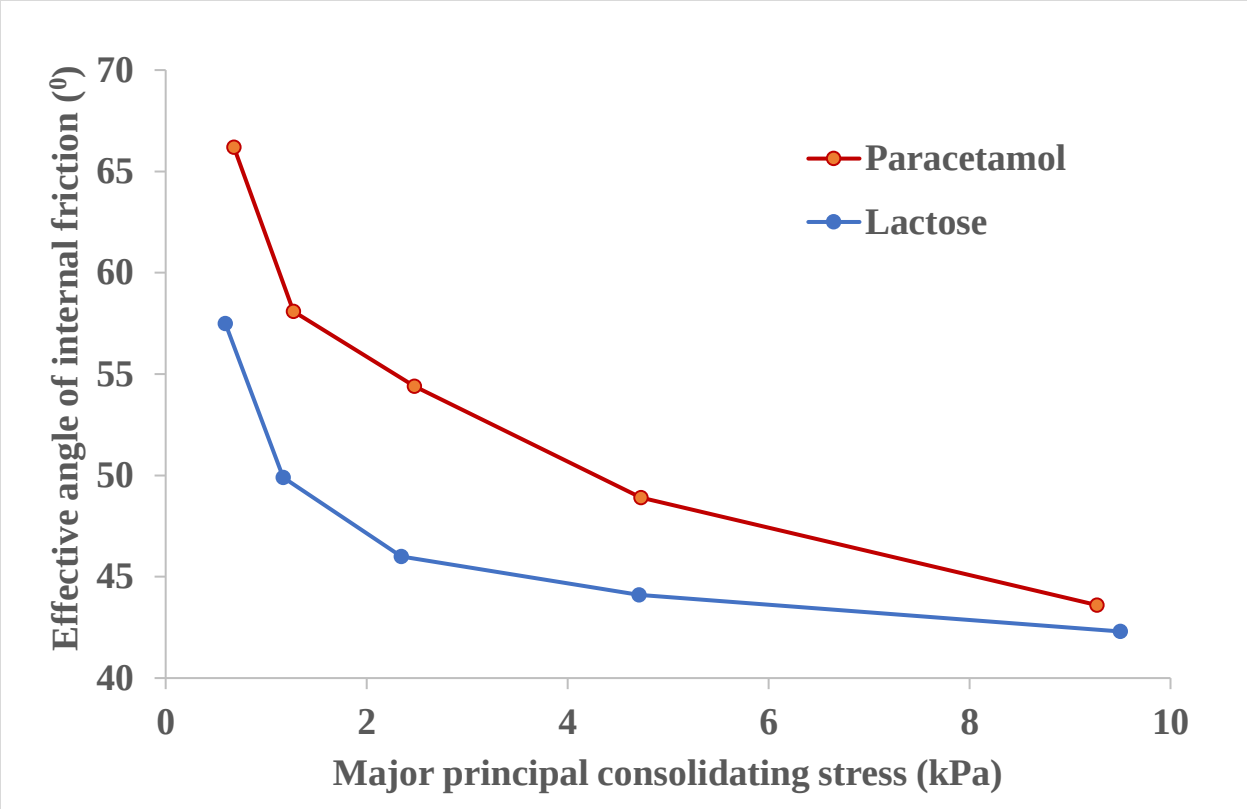

Figure 4.1.3: Effective angle of internal friction versus major consolidation stress for paracetamol and lactose samples

The effective angle of internal friction represents the relative contribution of adhesive forces to frictional forces. Figure 4.1.3 shows that the effective angle of internal friction values increase at lower consolidation stresses for both lactose and paracetamol, indicating that both the powders are of cohesive nature (Schulze, 2008). The reason for the decreasing nature of the trends with an increase in major consolidation stress is that although with the increase of major consolidation stress both the forces of particle to particle friction and adhesion increase simultaneously (as consolidation causes the particles to come closer to each other), but the increase of frictional forces between the particles caused due to enhanced surface to surface rubbing and interlocking is more dominant than the increase in adhesive forces (e.g. due to Van der Waals effect) (Schulze, 2008).

Due to this more dominant effect of frictional forces at high values of major principal consolidation stresses, the effective angle of internal friction decreases at higher major consolidation stress values. The reason for the paracetamol powders having higher values of effective angle of internal friction is that the paracetamol powders were having larger adhesive forces than lactose (due to the smaller particle size, larger specific surface area, irregular structure of paracetamol powders etc. compared to lactose, as explained in the previous section) and also as represented by Figure 4.1.2. Table 4.1.2 provides different states of experimental and stress conditions (some typical values) of instantaneous flow property testing.

Table 4.1.2: Sample test data for flow property testing for paracetamol and lactose powders

Consolidation endpoint	**Major principal consolidating stress**	**Unconfined failure strength**	**Gradient**	**Angle**	**Cohesion**	**Effective angle of internal friction**
(kPa)	(kPa)	(kPa)		(°)	(kPa)	(°)
Lactose						
0.306	0.594	0.477	0.44	23.6	0.156	57.5
0.603	1.17	0.757	0.51	26.9	0.233	49.9
1.201	2.345	1.216	0.57	29.6	0.354	46
2.407	4.712	2.093	0.6	30.8	0.595	44.1
4.843	9.501	3.627	0.61	31.3	1.019	42.3
Paracetamol						
0.3	0.679	0.596	0.53	28	0.179	66.2
0.596	1.273	1.016	0.47	25	0.323	58.1
1.195	2.475	1.829	0.48	25.7	0.574	54.4
2.402	4.73	2.97	0.51	26.8	0.913	48.9
4.839	9.269	4.713	0.51	27.1	1.441	43.6

Wall friction and bulk density tests

Figure 4.1.4 shows the trends of wall friction angles versus normal stress for paracetamol and lactose powders. Wall friction angle (φ_w) represents the friction between wall material and the powder layer adjacent to the walls at a given normal stress. The variation of wall friction angle with an increase in normal stress is shown in Figure 4.1.4.

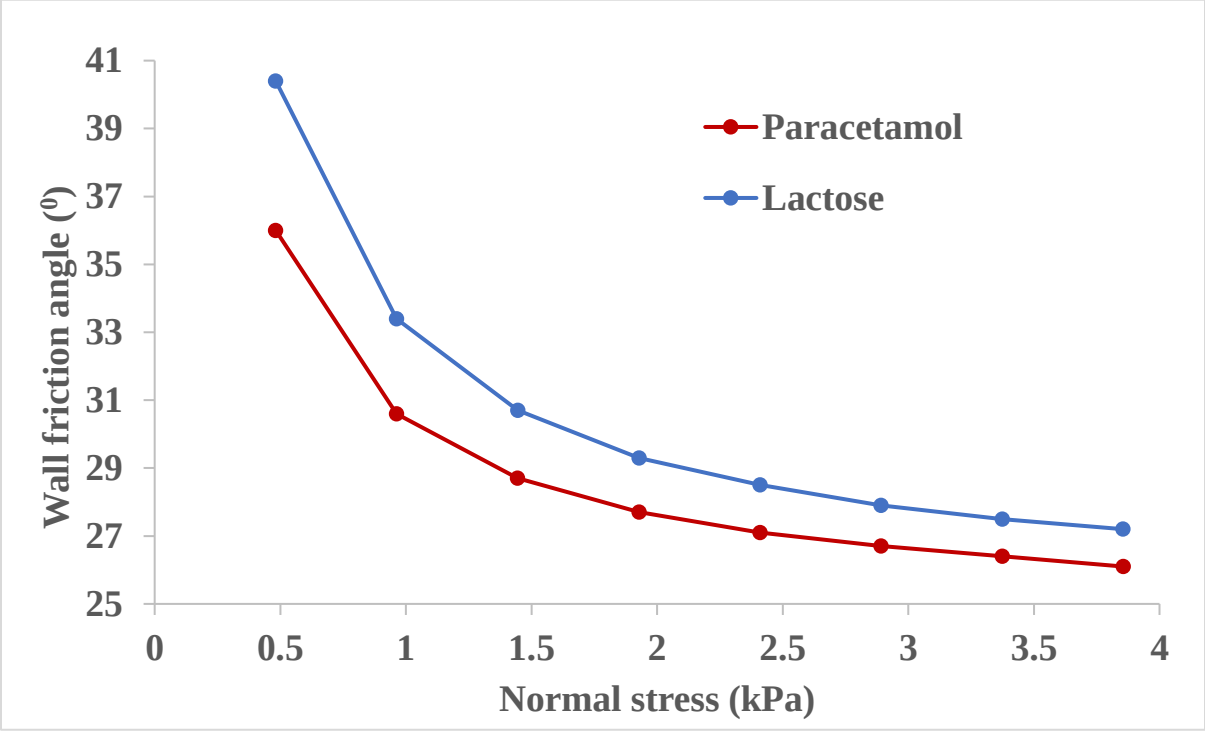

Figure 4.1.4: Trends of wall friction angle versus major consolidation stress for paracetamol and lactose powders

It can be seen from Figure 4.1.4 that the wall friction angle decreases with an increase in normal stress. Whereas the paracetamol powders were having smaller particle diameter and larger specific

surface area compared to lactose powders (which would contribute to higher adhesion and surface friction), the paracetamol powders on the contrary were having needle type irregular structure that would provide reduced contact surface of the particles with the wall (tending to reduce the friction at the wall). Practically it can be inferred from Figure 4.1.4 that the later effect (reduced wall friction due to reduced contact surface due to irregular shaped particles) seem to have played a more dominant role for paracetamol. Figure 4.1.5 shows the variation of bulk density with an increase in normal stress for paracetamol and lactose powders.

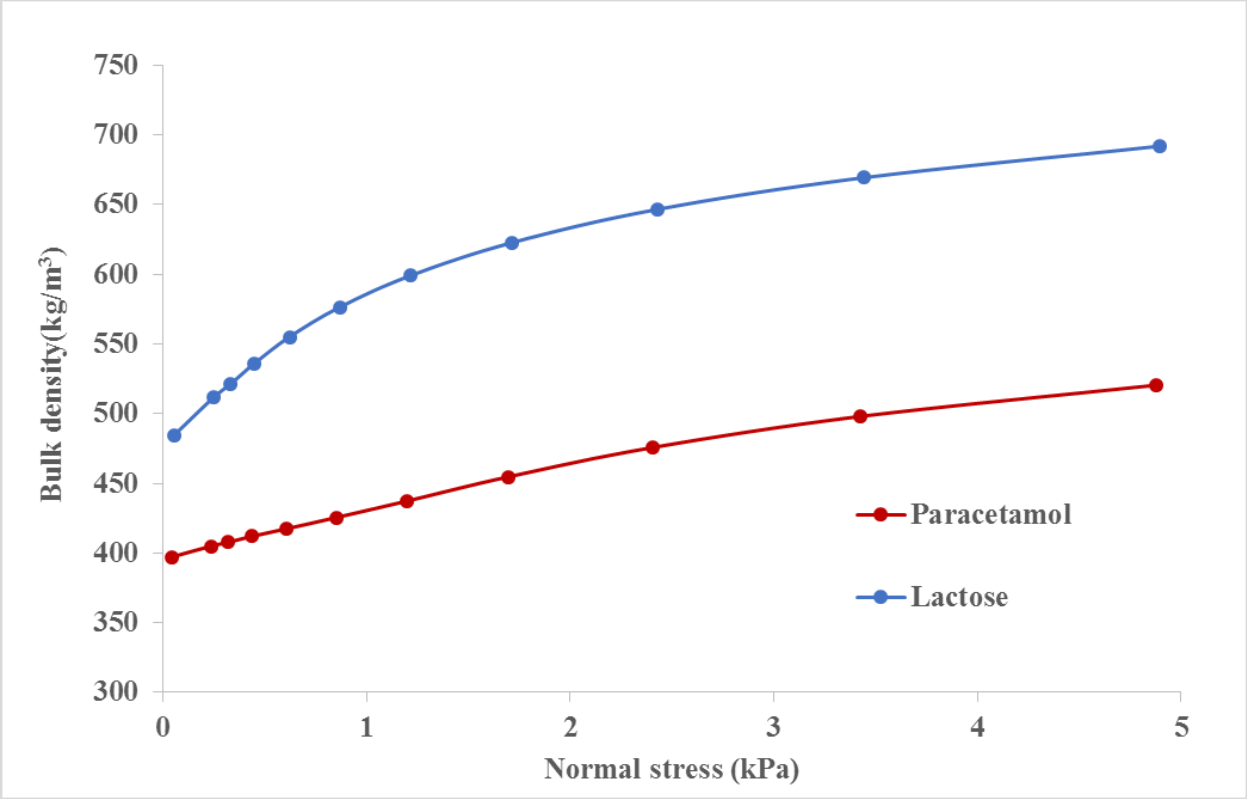

Figure 4.1.5: Bulk density versus normal stress for paracetamol and lactose powders

Figure 4.1.5 shows that the trends of bulk density versus normal stress for both the powders follow a sharp rising curve at low stress. Following this, the curves tend to get flatten towards the higher

stress values. The reduction of slope at higher normal stress is more prominent for lactose than paracetamol. This is because the paracetamol powders were having lower bulk density and higher porosity than lactose. Hence, the paracetamol powders could be compressed to a greater extent before further addition of load would result in increase in bulk density at a reduced rate. On the contrary, the voidage of the lactose powders were initially low and thereafter on addition of load, the lactose powders showed the tendency of attaining lower rate of rise of bulk density (change in trend) at a load that is considerably lower than that of paracetamol.

Time consolidation tests

Some bulk solids gain additional strength if stored at rest under compressive stress for a long-time of period, e.g. powders stored overnight or over the weekend or during the shutdown condition in a plant. This effect is known as time consolidation (Schulze, 2008). Gain in strength over time is caused by visco-plastic or plastic deformation at particle contacts leading to an increase in adhesive forces due to the reduction of distance between the particles and enlargement of contact areas, formation of solid bridges due to solid crystallizing when drying moist bulk solids etc. (Schulze, 2008). In these tests, the sample was subjected to static load (i.e. it was not sheared) for a time span is 12 hours, because generally these powders (lactose and paracetamol) are stored overnight in plants. Table 4.1.3 and 4.1.4 compare the unconfined yield stress for lactose and paracetamol powders before and after time consolidation for different pre-shear conditions.

Table 4.1.3: Unconfined yield strength for lactose powder before and after time consolidation

Sample	σ_c at σ_{pre1} kPa	σ_c at σ_{pre2} kPa	σ_c at σ_{pre3} kPa	σ_c at σ_{pre4} kPa	σ_c at σ_{pre5} kPa
Lactose (before time consolidation test)	0.257	0.568	0.911	1.606	2.648.
Lactose (after time consolidation test)	0.853	1.327	1.869	3.398	4.915

Table 4.1.4: Unconfined yield strength for paracetamol powder before and after time consolidation

Sample	σ_c at σ_{pre1} kPa	σ_c at σ_{pre2} kPa	σ_c at σ_{pre3} kPa	σ_c at σ_{pre4} kPa
Paracetamol (before time consolidation test)	0.661	0.887	1.694	2.447
Paracetamol (after time consolidation test)	1.461	1.993`	3.536	5.115

A comparison of unconfined yield strength values before and after time consolidation provided in Table 4.1.3 and 4.1.4 show that both the powders gain strength (increase in unconfined yield stress) after time consolidation. Figure 4.1.6 shows the trends of unconfined yield strength to major consolidation stress for lactose after time consolidation. For the purpose of demonstrating the gain in strength, instantaneous flow function curves have been superimposed. Figure 4.1.6 reveals that the lactose powders have become “very cohesive” after time consolidation from being “easy

flowing"/ "cohesive" before time consolidation; the paracetamol powders have become "very cohesive" after time consolidation from being "easy flowing"/ "cohesive" before time consolidation.

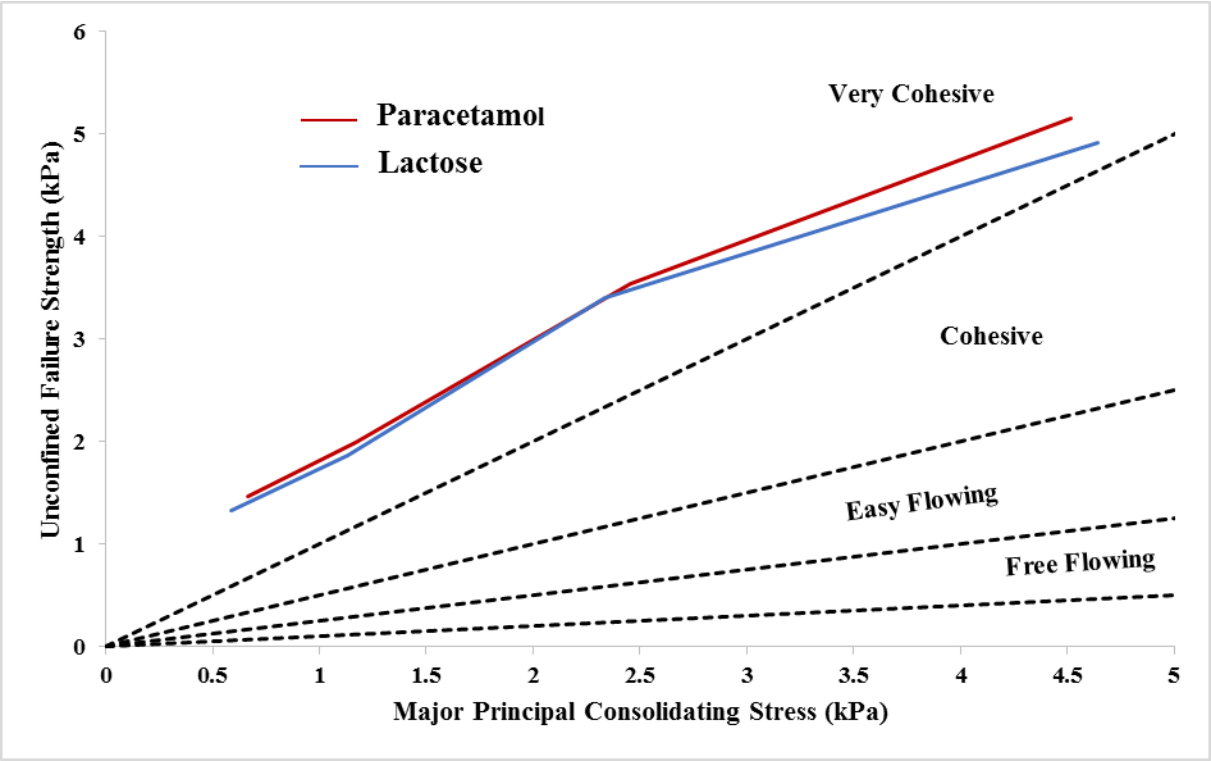

Figure 4.1.6: Flow function curves for paracetamol and lactose powders based on time consolidation test results

Critical dimensions of mass flow hopper

Hopper half angle (θ) and outlet opening (D) are the critical parameters for hopper design, especially if mass flow condition is to be ensured. Jenike (Jager et al, 2015) did pioneering work by deriving mathematical relations between hopper critical dimensions and powder flow properties. Using the results obtained from flow property and wall friction tests, hopper half angles

and critical outlet openings were determined from equations (4.1.5) and (4.1.6) by using flow properties found at different pre-shear stresses. The results are shown in Figure 4.1.7.

$$D = \frac{2\ X\ \sigma_c\ X\ 1000}{\rho_b\ X\ g} \tag{4.1.5}$$

$$\theta = \left[90 - \frac{1}{2}\cos^{-1}\left(\frac{1-\sin\delta}{2\sin\delta}\right)\right] - \frac{1}{2}\left[\varphi_w + \sin^{-1}\left(\frac{\sin\varphi_w}{\sin\delta}\right)\right] \tag{4.1.6}$$

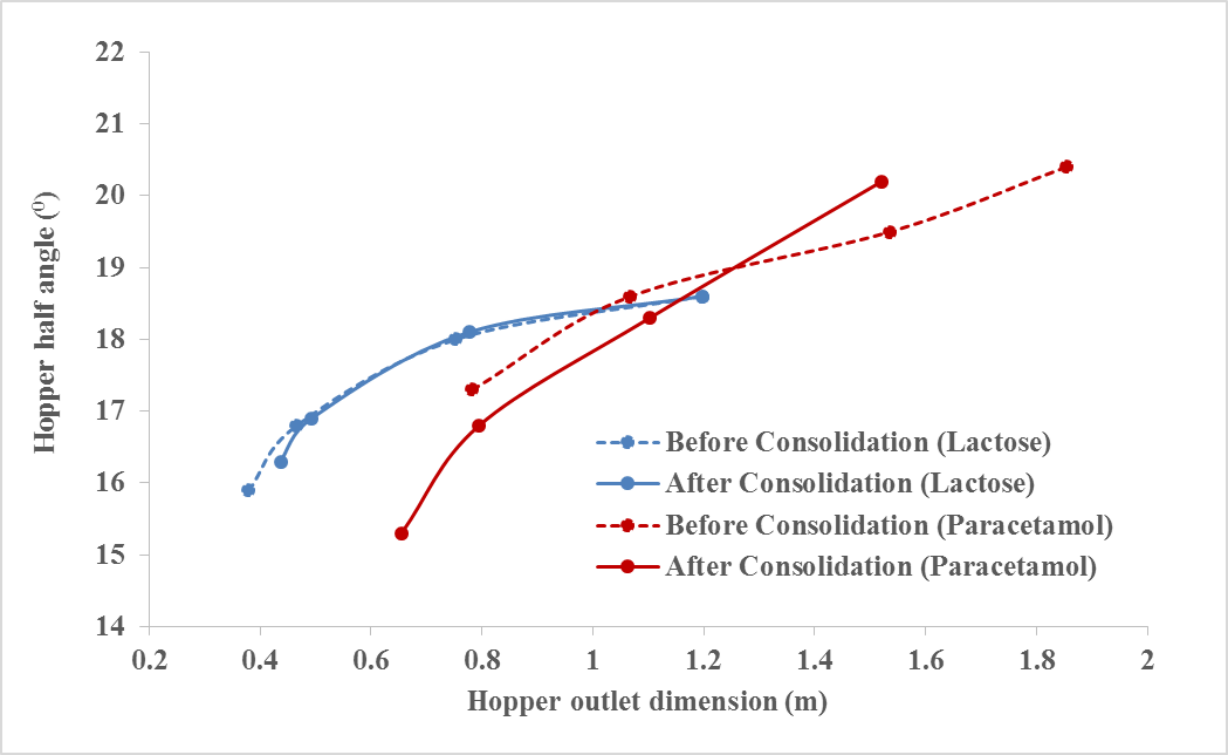

Figure 4.1.7: Comparison of hopper half angle to outlet dimension for lactose and paracetamol powders with and without time consolidation effects

Figure 4.1.7 shows that the paracetamol powder being relatively more cohesive than lactose for both instantaneous and time consolidation cases, would require wider hopper outlet dimensions

than the lactose powders. Also, it can be seen that time consolidation has a strong effect on paracetamol, where a considerable amount of additional hopper outlet size is required (for the same hopper angle) to accommodate the effect of time consolidation. Surprisingly, the results show that 12 hrs of consolidation are inadequate to cause any considerable difference in the flow behavior (or design parameters, such as requirement of hopper outlet size) for lactose powders, where the without and with time consolidation trends are almost over-lapping each other. The results show that the higher hopper angle would require a larger hopper opening and the trend is sharper in case of paracetamol powders than lactose.

4.2 Results and discussion for Calcium Sulphate and Di-Calcium Phosphate

4.2.1 Physical properties of powders

Table 4.2.1 provides the various physical properties of calcium sulphate and di-calcium phosphate powders. Figure 4.2.1 shows the Scanning Electron Microscopy (SEM) images of calcium sulphate and di-calcium phosphate powders. Table 4.2.1 shows that the average particle size of di-calcium phosphate powders is less than that of calcium sulphate powders. This indicates the presence of more fines in di-calcium phosphate. As a result, the specific surface area is more for di-calcium phosphate powders (as shown in Table 4.2.1). Smaller particle size and the presence of more fines in case of di-calcium phosphate would cause larger amounts of Van der Waals forces of attraction (adhesion) amongst the particles (Amagliani et al., 2016). Additionally, larger specific surface area of dicalcium phosphate powders would cause greater surface resistance (Amagliani et al., 2016). The Hausner ratio value of di-calcium phosphate is larger than calcium sulphate. This indicates that the di-calcium phosphate powders can be compressed to relatively larger tapped density than

calcium sulphate powders. This further points out that the di-calcium phosphate powders have stronger particle-particle cohesion and as a result, it would exhibit poor flowability compared to the calcium sulphate powders. The contributing factor for achieving relatively larger tapped density for di-calcium phosphate is that the di-calcium phosphate powders were having larger particle to particle air gaps (greater amount of porosity) under the loose poured condition. (Abdullah and Geldart, 1999). Therefore, when tapped, the dicalcium phosphate powders could occupy those void spaces more readily than the calcium sulphate powders, which were having relatively lesser amount of void spaces under the loose poured condition. As a result, the calcium sulphate powder had lesser amount of void spaces for the fines to occupy under the application of tapping. The results of particle size, surface area, Hausner ratio and porosity all indicate that the di-calcium phosphate powders are likely to be a poorer flowable powder compared to calcium sulphate powders. Span was determined using equation 4.2.1 to evaluate the range of size distribution.

$$\text{Span} = (d_{90}-d_{10})/d_{50} \quad (4.2.1)$$

Where, d_{50} is defined as the diameter below which half of the powder population lies. Similarly, 10 and 90% of the distribution lies below the size values of d_{10} and d_{90}, respectively.

Porosity (Li et al, 2016) and compressibility index (Ji et al, 2017) were calculated using the following formulae:

$$\text{Porosity} = 1- (\rho_{lb}/\rho_p) \quad (4.2.2)$$

$$\text{Compressibility Index} = 100 \times [1- (\rho_{lb}/\rho_t)] \quad (4.2.3)$$

Table 4.2.1: Physical properties of calcium sulphate and di-calcium phosphate

Powders	**d_{10} (µm)**	**d_{50} (µm)**	**d_{90} (µm)**	**ρ_{lb} (kg/m^3)**	**ρ_p (kg/m^3)**	**ρ_t (kg/m^3)**	**Hausner Ratio (HR)**	**CI**	**Porosity**	**Span**	**SSA (m^2/kg)**
Calcium sulphate	9	47	73	776	2500	921	1.186	15.75	0.689	1.361	152
Di-calcium phosphate	7	23	64	964	3333	1316	1.365	26.75	0.711	2.478	225

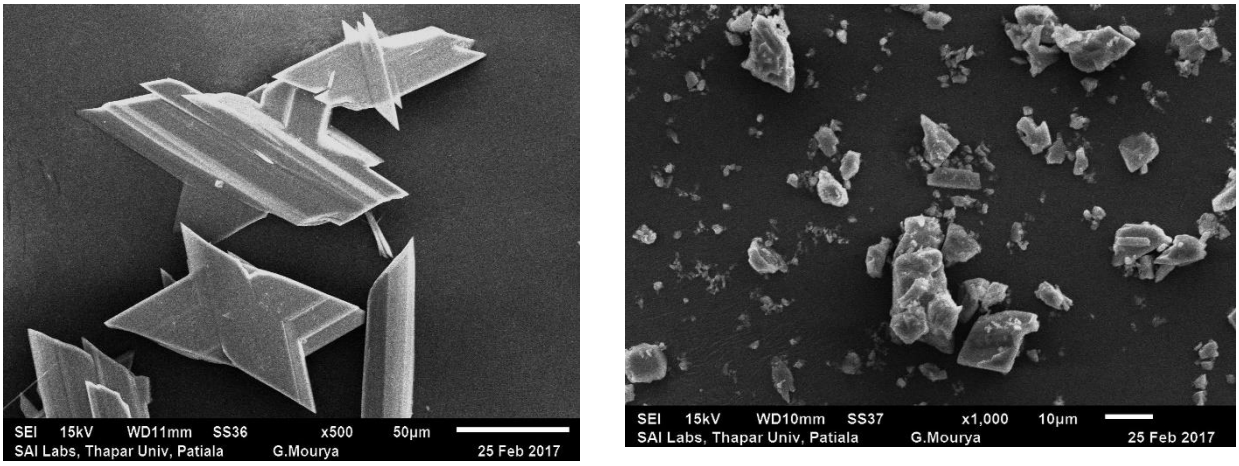

(a) Calcium Sulphate Sample (b) Dicalcium Phosphate Sample

Figure 4.2.1: SEM images of calcium sulphate and di-calcium phosphate samples

4.2.2 Flow properties of calcium sulphate and di-calcium phosphate powders

Yield locus and flow function curves

Yield locus of powders represents the shear stress (τ) necessary to initiate the flow in the powder sample under a given consolidation stress (σ) (Jager et al., 2015). Yield locus is a curve which is generated between normal consolidation stress and shear stress and can be represented by the equation 4.2.4 at any given pre-shear condition.

$$\tau = \sigma \tan \varphi + C \qquad (4.2.4)$$

Where, φ is the internal friction angle representing the magnitude of friction between the layers of powder. The values of pre-shear stresses for calcium sulphate were 0.310, 0.608, 1.205, 2.410 and 4.847 kPa, whereas the same for dicalcium phosphate powders were 0.316, 0.614, 1.214, 2.421 and 4.859 kPa, respectively. Each yield locus provides major consolidation stress (σ_1) and the corresponding values of unconfined yield strength (σ_c) related to the powder. Figure 2 shows the flow function curve (a plot between σ_1 and σ_c) for di-calcium phosphate and calcium sulphate. The flow function curve (Figure 4.2.2) has been divided in four parts based on Jenike's flowability classification (Jager et al., 2015)., as reported by Saw et al. (2015). Flow Index (FI) is the reciprocal of flow function curve slope (σ_1/σ_c) and indicates the relative flowability of the powders. Typical values of Flow Index (FI) and the slope of flow function curve for calcium sulphate at a pre-shear value of 1.2 kPa were 3.802 and 0.13, respectively. Values of the same parameters under the same pre-shear condition for di-calcium phosphate were 1.933 and 0.32, respectively. Figure 4.2.2 shows that below the major principal consolidation stress of about 2.5 kPa, the di-calcium phosphate powders fell in the "cohesive" regime. However, above this consolidation stress, this powder fell into the "easy flowing" regime. On the other side, the calcium sulphate powders remained in the "easy flowing" regime up to a consolidation stress of 3.2 kPa and beyond this stress, it entered into the "free flowing" range. The reason for di-calcium phosphate being more cohesive compared to calcium sulphate powder has been already explained in the previous section. Figure 4.2.2 is based on instantaneous flow function results.

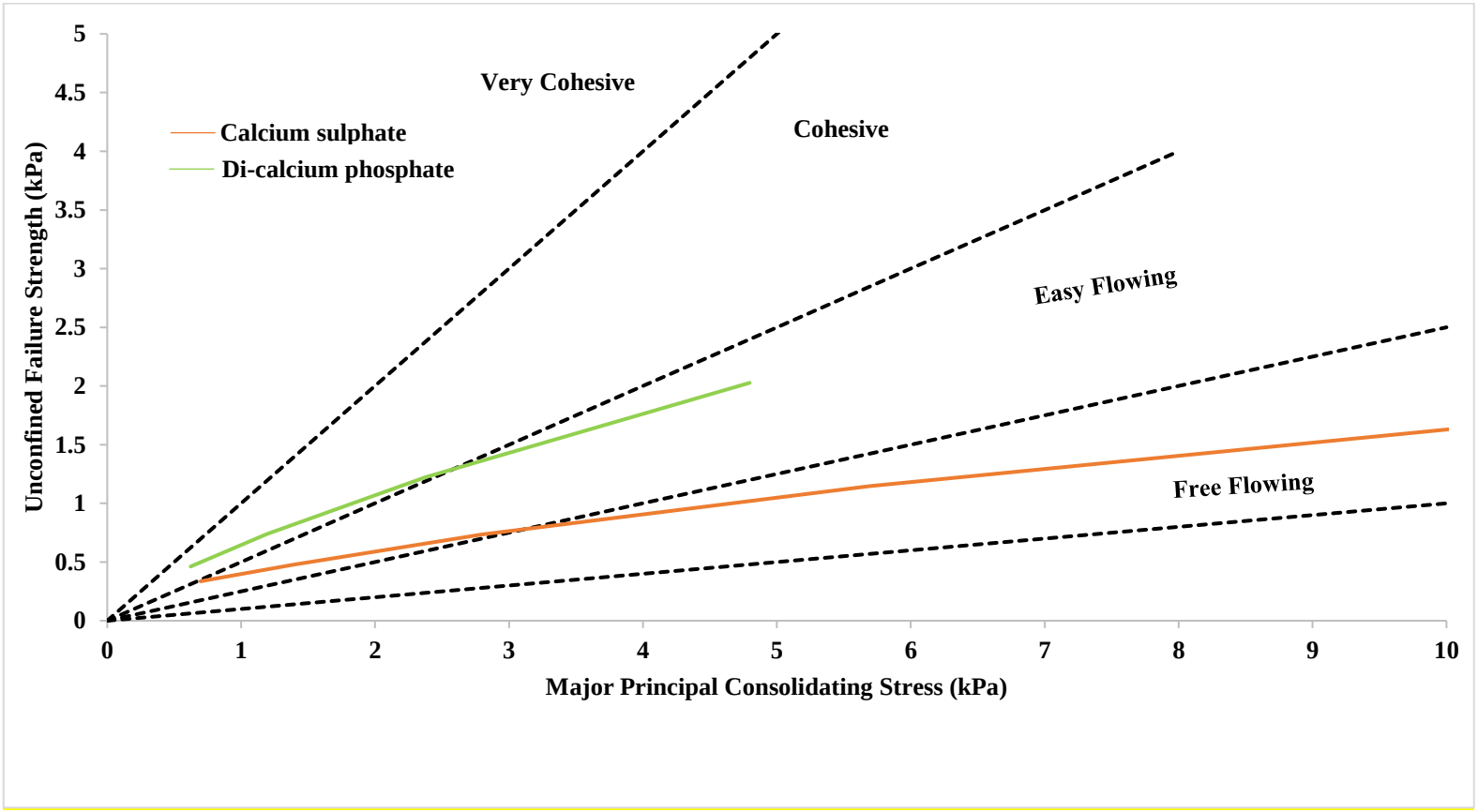

Figure 4.2.2: Flow function curves for calcium sulphate and di-calcium phosphate based on instantaneous flow function test results

Effective angle of internal friction (δ) is the ratio of major consolidation and minor consolidation stresses over the powder element in steady state flow (Jenike, 1964). The trend of variation of effective angle of internal friction with major consolidation stress is given in Figure 4.2.3.

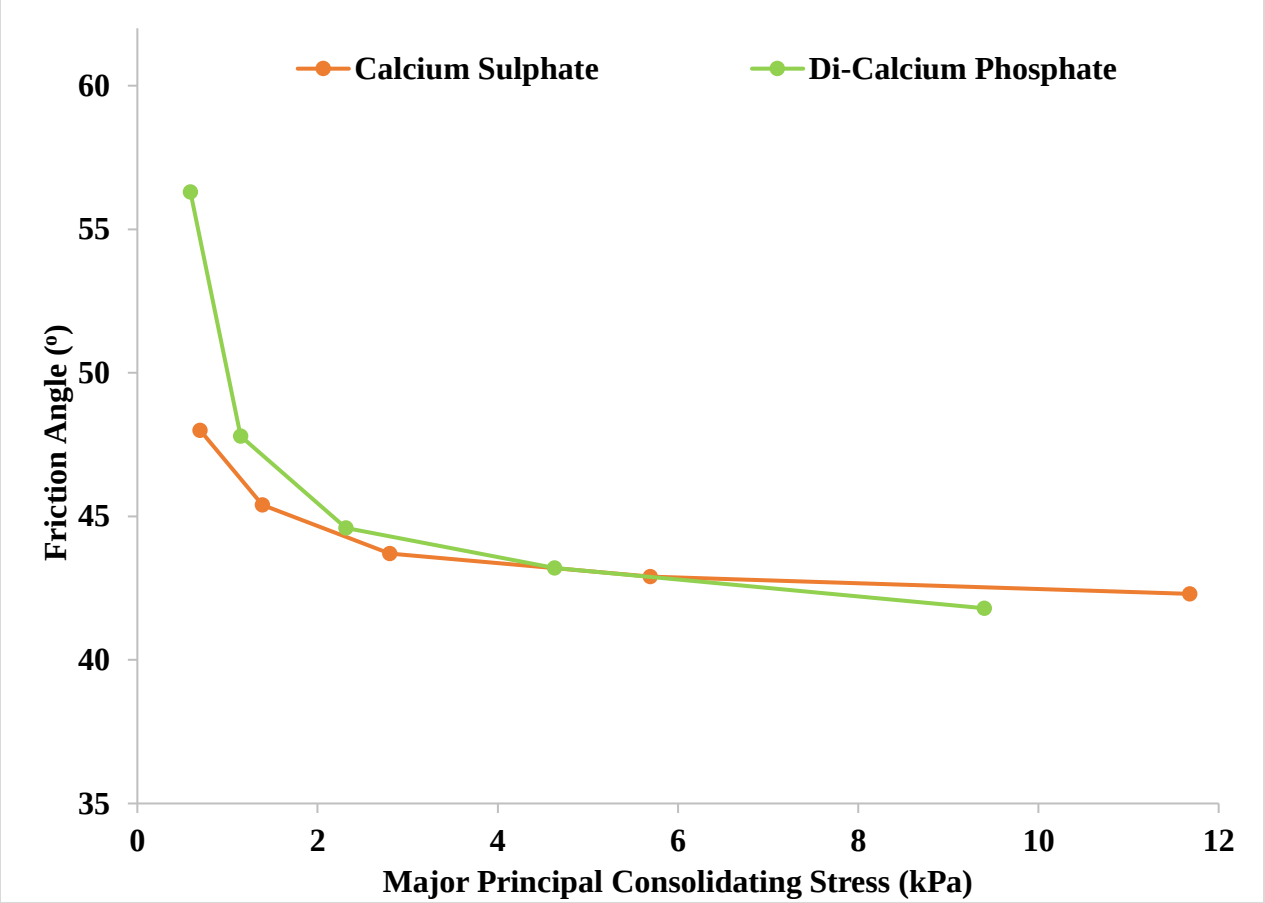

Figure 4.2.3: Effective angle of internal friction versus major consolidation stress for di-calcium phosphate and calcium sulphate

The effective angle of internal friction of powders represents the relative contribution of adhesive forces to frictional forces. Figure 4.2.3 shows that the effective angle of internal friction values are larger at lower consolidation stresses for both the powders. The increment is considerably larger

for di-calcium phosphate indicating that this powder is more cohesive than calcium sulphate (Schulze, 2008). The reason for the di-calcium phosphate powders having higher values of effective angle of internal friction is that the dicalcium phosphate powders were having larger adhesive forces than calcium sulphate (due to the smaller particle size, larger specific surface area, irregular structure of dicalcium phosphate powders etc. compared to calcium sulphate, as explained in the previous section) and also as represented by Figure 4.2.2. The reason for the decreasing nature of the slopes with increasing values of major consolidation stress is that although both the forces of particle to particle friction and adhesion increase simultaneously (as consolidation causes the particles to come closer to each other) with the increase of major consolidation stress, but the increase of frictional forces between the particles caused due to enhanced surface to surface contact friction and interlocking is far greater than the increase in adhesive forces, such as the Van der Waals effect (Schulze, 2008). As a result of larger prevalence of frictional forces at larger values of major principal consolidation stresses, the effective angle of internal friction decreases at higher major consolidation stresses. Table 4.2.2 provides different states of stress conditions with some typical values of instantaneous flow property testing.

Table 4.2.2: Sample test data for flow property testing for calcium sulphate and di-calcium phosphate

Consolidation endpoint (kPa)	**Major principal consolidating stress (kPa)**	**Unconfined failure strength (kPa)**	**Gradient**	**Angle (°)**	**Cohesion (kPa)**	**Effective angle of internal friction (°)**
Calcium sulphate						
0.31	0.696	0.336	0.67	33.8	0.09	48
0.608	1.387	0.478	0.73	36.3	0.121	45.4
1.205	2.8	0.735	0.76	37.1	0.183	43.7
2.41	5.692	1.147	0.78	38	0.28	42.9
4.847	11.68	1.817	0.8	38.6	0.437	42.3
Di-calcium phosphate						
0.316	0.589	0.47	0.41	22.1	0.158	56.3
0.614	1.147	0.725	0.47	25	0.231	47.8
1.214	2.314	1.197	0.53	27.9	0.361	44.6
2.421	4.63	2.033	0.58	30	0.587	43.2
4.859	9.399	3.347	0.62	31.7	0.933	41.8

Wall friction and bulk density tests

Figure 4.2.4 shows the trends of wall friction angles versus normal stress for di-calcium phosphate and calcium sulphate powders. The friction between wall material and the powder layer adjacent to the walls at a given normal stress is given by wall friction angle (φ_w).

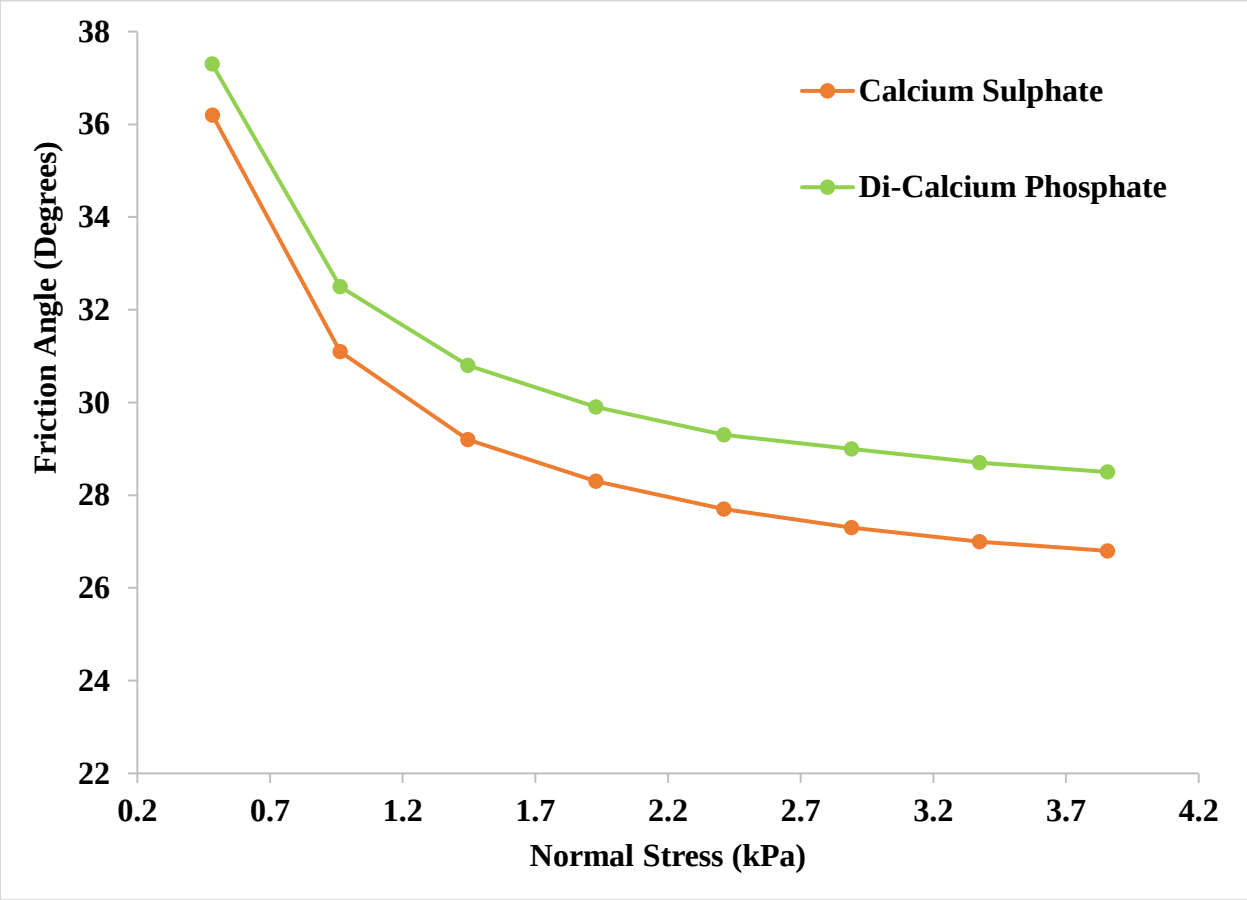

Figure 4.2.4: Trends of wall friction angle versus major consolidation stress for dicalcium phosphate and calcium sulphate powders

It can be seen from Figure 4.2.4 that the wall friction angle decreases with an increase in normal stress. The di-calcium phosphate powders were having smaller particle diameter and larger specific surface area compared to calcium sulphate powders. This would cause higher adhesion and surface friction for the case of di-calcium phosphate due to more particle surface to wall contact. Figure 4.2.5 shows the variation of bulk density with an increase in normal stress for dicalcium phosphate and calcium sulphate powders. The trends of bulk density versus normal stress for both the powders follow a relatively sharper rising curve at low normal stress values. After the initial sharp rise, the curves tend to get flatten out in the higher stress value ranges.

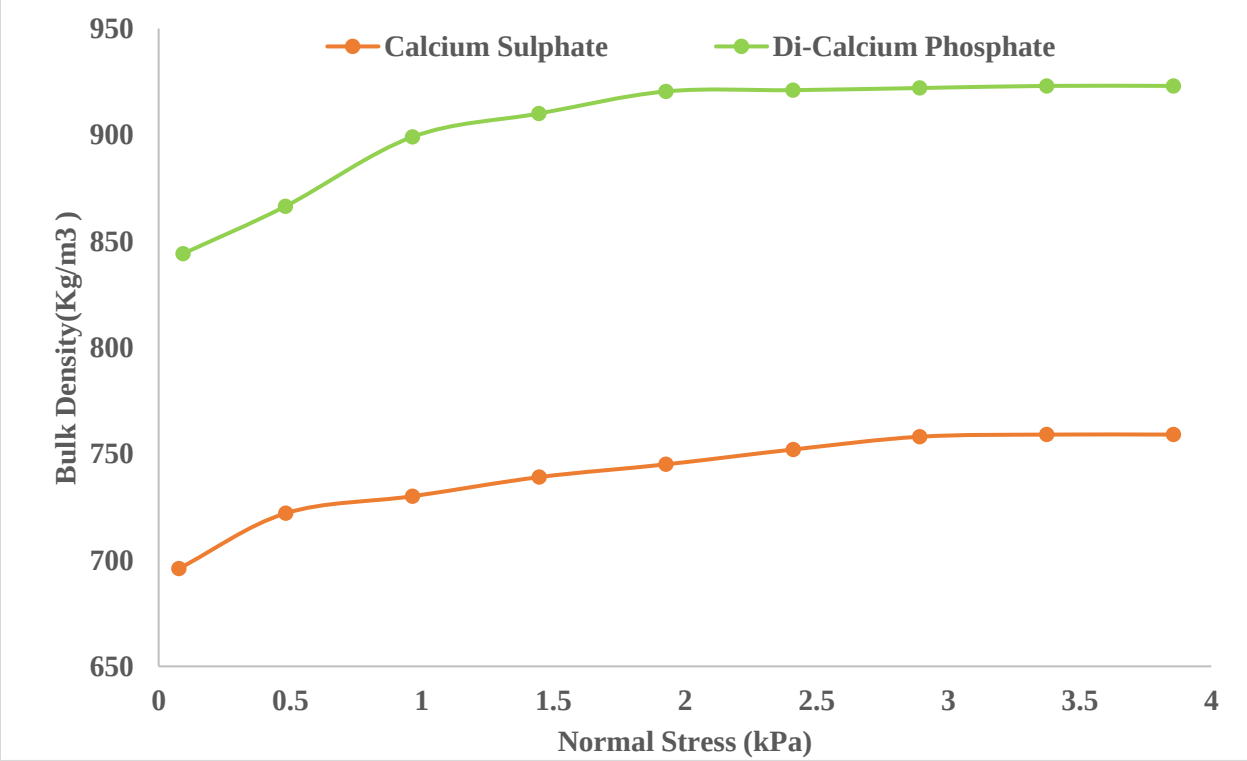

Figure 4.2.5: Bulk density versus normal stress for di-calcium phosphate and calcium sulphate powders

Time consolidation tests

Certain bulk powders gain additional strength when stored at rest under compressive stress for a long-time period. This effect is known as time consolidation (Schulze, 2008). This may happen when the powders are stored overnight or over the weekend or during the shutdown condition in a plant, e.g. pharmaceutical industry. Gain in strength due to time consolidation is caused by visco-plastic or plastic deformation at particle contact zones resulting in the enhancement of adhesive forces due to the shortening of distance between the particles and increase in contact areas, development of solid bridges due to solid crystallization during the drying of moist bulk solids etc. (Schulze, 2008). In time consolidation tests, the sample was subjected to a static load (i.e. it was not sheared) for a time span is 12 hours. This time frame was kept as generally these powders (calcium sulphate and dicalcium phosphate) are stored overnight in pharmaceutical industries. Table 4.2.3 and 4.2.4 compare the unconfined yield stress for calcium sulphate and dicalcium phosphate powders before and after time consolidation under different pre-shear stress applications.

Table 4.2.3: Unconfined yield strength for calcium sulphate before and after time consolidation

Sample	**σ_c at σ_{pre1} kPa**	**σ_c at σ_{pre2} kPa**	**σ_c at σ_{pre3} kPa**	**σ_c at σ_{pre4} kPa**	**σ_c at σ_{pre5} kPa**
Calcium Sulphate (before time consolidation test)	0.336	0.478	0.735	1.147	1.817
Calcium Sulphate (after time consolidation test)	0.498	0.684	0.932	1.398	2.306

Table 4.2.4: Unconfined yield strength for di-calcium phosphate before and after time consolidation

Sample	**σ_c at σ_{pre1} kPa**	**σ_c at σ_{pre2} kPa**	**σ_c at σ_{pre3} kPa**	**σ_c at σ_{pre4} kPa**
Dicalcium Phosphate (before time consolidation test)	0.462	0.738	1.224	2.027
Dicalcium Phosphate (after time consolidation test)	0.544	0.863`	1.281	1.933

A comparison of unconfined yield strength results before and after time consolidation (Table 4.2.3 and 4.2.4 show) that both the powders gained additional strength after time consolidation. Figure

4.2.6 presents flow function curves for calcium sulphate and di-calcium phosphate after time consolidation. Figure 4.2.6 reveals that the calcium sulphate powders have become “cohesive” at low stresses after time consolidation from being “easy flowing” before time consolidation; the di-calcium phosphate powders have continued to remain in “cohesive” zone (but with a greater portion inside the “cohesive regime compared to the instantaneous flow function results).

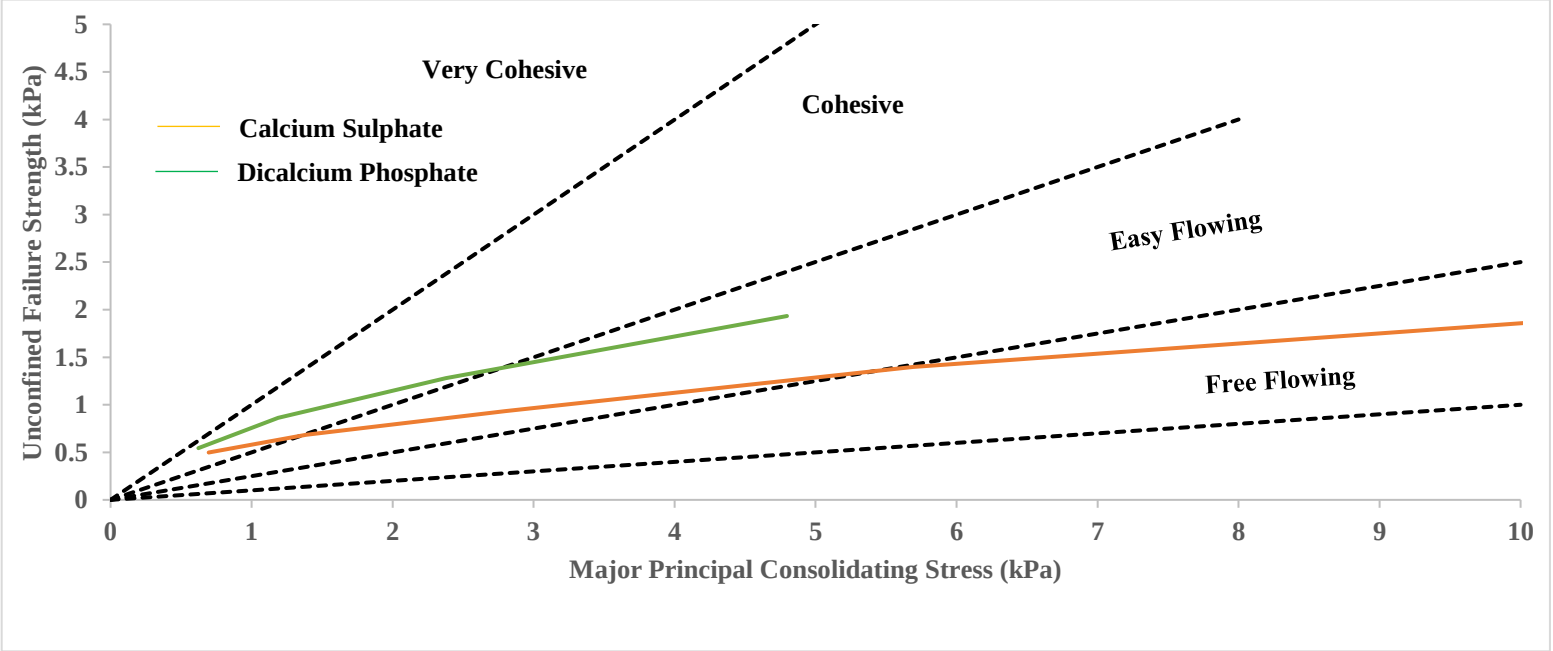

Figure 4.2.6: Flow function curves for di-calcium phosphate and calcium sulphate powders based on time consolidation test results

Critical dimensions of mass flow hopper

Hopper half angle (θ) and outlet opening (D) are the critical parameters for hopper design especially to maintain reliable mass flow of powders. Jenike, A.W., 1964, carried out pioneering work by deriving mathematical relations powder flow properties. Hopper half angles and critical outlet openings were determined from equations (4.2.5) and (4.2.6) by using the results obtained from flow property and wall friction tests (corresponding to instantaneous and time consolidation tests). The results are shown in Figure 4.2.7.

$$D = \frac{2\ X\ \sigma_c\ X\ 1000}{\rho_b\ X\ g} \tag{4.2.5}$$

$$\theta = \left[90 - \frac{1}{2}\cos^{-1}\left(\frac{1-\sin\delta}{2\sin\delta}\right)\right] - \frac{1}{2}\left[\varphi_w + \sin^{-1}\left(\frac{\sin\varphi_w}{\sin\delta}\right)\right] \tag{4.2.6}$$

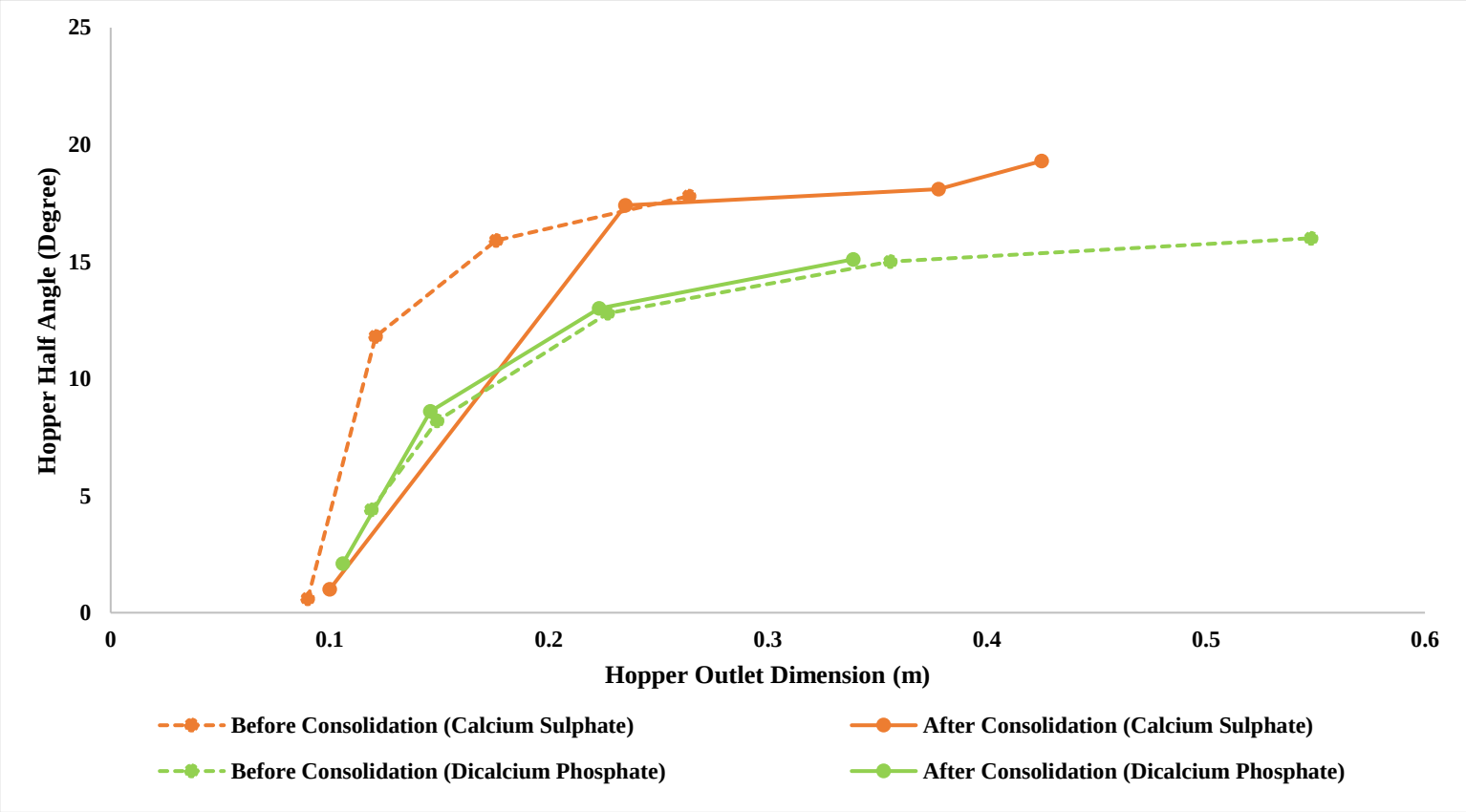

Figure 4.2.7: Comparison of hopper half angle to outlet dimension for calcium sulphate and di-calcium phosphate powders with and without time consolidation effects

Figure 4.2.7 shows that the di-calcium phosphate powder would require wider hopper outlet dimensions compared to the calcium sulphate powders. This is due to the larger cohesion in case of di-calcium phosphate powders. Also, it is found that time consolidation has a stronger effect on calcium sulphate. For this powder, a considerable amount of additional hopper outlet size is required (for the same hopper angle) after time consolidation compared to the requirement outlet openings obtained from instantaneous test results. The results indicate that 12 hrs. of consolidation time are inadequate to result in any considerable difference in the flow behavior (or design of hopper dimensions) for di-calcium phosphate powders.

4.3 Results and discussion for Magnesium Tri-Silicate and Starch

4.3.1 Physical properties of powders

Table 4.3.1 lists the various physical properties of Magnesium Tri-Silicate and Starch. Figure 4.3.1 shows the Scanning Electron Microscopy (SEM) images of Magnesium Tri-Silicate and Starch powders. Table 4.3.1 shows that the average particle size of Starch powders is less than that of Magnesium Tri-Silicate powders, indicating the presence of more fines in Starch powders. As a result, the specific surface area is also more for Starch powders (Table 4.3.1). Smaller particle size and the prevalence of more fines would tend to result in larger amounts of Van der Waals forces of attraction (adhesion) amongst the particles in case of Starch powders (Amagliani et al., 2016). However, the SEM images provided in Figure 4.3.1 shows that the Starch powders were having relatively more uniform and smooth shapes compared to the Magnesium Tri-Silicate powders (Li et al., 2016). Though not precisely spherical, but the Starch powders seem to have similar

dimensions of length to width (and hence, closer to having a spherical shape) compared to Magnesium Tri-Silicate powders. Compared to the Starch powders, the Magnesium Tri-Silicate powders seem to have a more irregular appearance. It is believed that the more the structure is shaped irregular (away from spherical), the more would be the resistance of the powders to flow under disturbance (such as tapping) or under compressive load. This is due to the fact that the spherical or closer to spherical shaped particles with relatively smoother surface (such as Starch) would move against each other more easily compared to irregular shaped particles such as Magnesium Tri-Silicate, where the particles would experience greater frictional resistance to flow pass each other contributed by larger surface roughness. However, on the contrary, larger specific surface area of Starch powders would contribute to increased surface resistance (Amagliani et al., 2016). Therefore, while smaller particle size and larger specific surface area of Starch would point to Starch being relatively more cohesive, on the contrary the more uniform (and closer to spherical) shaped Starch powders tends to indicate that the starch powders would flow better under load due to reduced surface roughness. Generally, a lower value of loose poured bulk density and higher value of tapped density are indicative of a more cohesive powder. Greater particle-particle adhesion would cause powders to not settling down easily under gravity by not moving against each other and experiencing lesser relative realignment in position and orientation under load (Amagliani et al., 2016). On the contrary, the lack of cohesion amongst the particles tend to result in higher bulk density as the particles are relatively freer to move against each other, reorient and occupy interparticle void spaces (Amagliani et al., 2016). For the case of Starch and Magnesium Tri-Silicate, due to their contrasting characteristics, it would not be easy to theoretically predict based on only the physical property testing that which powder will be relatively more cohesive under actual flow conditions (practical conditions). Whereas the starch powders are smaller in size,

exhibiting more specific surface area and having larger porosity (all of which point towards Starch would be more cohesive and difficult to flow), the Starch powders also exhibit smaller Hausner ratio values and more uniform and smooth shape, respectively (pointing towards starch could have a tendency of being easier flowing). Due to these contrasting and inconclusive findings obtained from the physical characterization tests, it was thought that relying on the practical results of flow property testing for both the powders for hopper design would be more direct, reliable and credible. Span was determined using equation 4.3.1 to evaluate the range of size distribution.

$$\text{Span} = (d_{90}-d_{10})/d_{50} \quad (4.3.1)$$

Where, d_{50} is defined as the diameter below which half of the powder population lies. Similarly, 10 and 90% of the distribution lies below the size values of d_{10} and d_{90}, respectively.

Porosity (Li et al, 2016) and compressibility index (Ji et al, 2017) were calculated using the following formulae:

$$\text{Porosity} = 1- (\rho_{lb}/\rho_p) \quad (4.3.2)$$

$$\text{Compressibility Index} = 100 \times [1- (\rho_{lb}/\rho_t)] \quad (4.3.3)$$

Table 4.3.1: Physical properties of Magnesium Tri-Silicate and Starch

Powders	**d_{10} (µm)**	**d_{50} (µm)**	**d_{90} (µm)**	**ρ_{lb} (kg/m^3)**	**ρ_p (kg/m^3)**	**ρ_t (kg/m^3)**	**HR**	**CI**	**Porosity**	**Span**	**SSA (m^2/kg)**
Magnesium Tri-Silicate	5	33	52	422	1428	562	1.33	24.91	0.7044	1.424	219
Starch	3	21	41	546	2000	715	1.31	23.63	0.7270	1.809	254

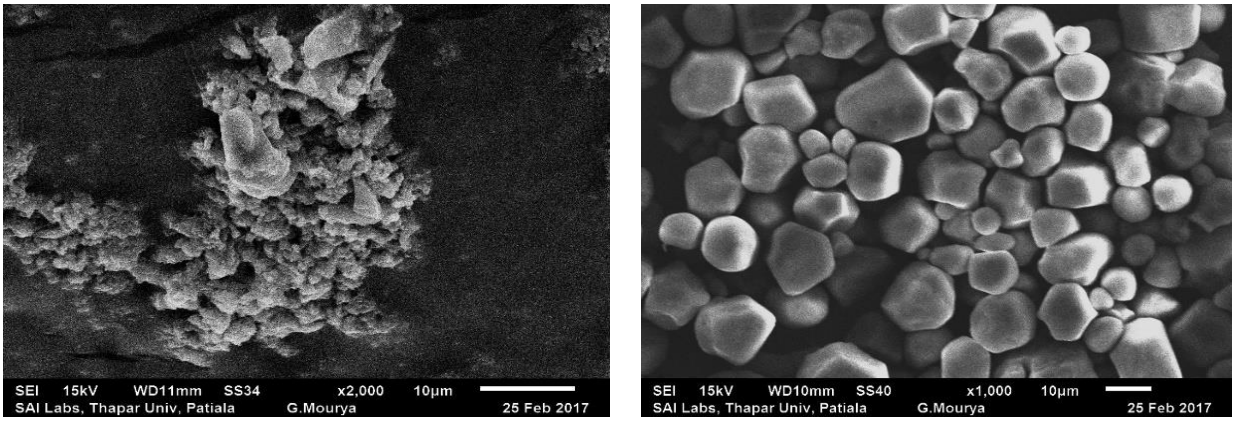

(a) Magnesium Tri-Silicate (b) Starch

Figure 4.3.1: SEM Images of Magnesium Tri-Silicate and Starch samples

4.3.2 Flow properties of Magnesium Tri-Silicate and Starch powders

Yield locus and flow function curves

Yield locus of powder sample signifies the shear stress (τ) necessary to initiate the flow under a given consolidation stress (σ) (Schulze, 2008). Yield locus is a plot which is generated between normal consolidation stress and shear stress and can be represented by equation 4.3.4.

$$\tau = \sigma \tan \varphi + C \qquad (4.3.4)$$

Where, φ is the angle of internal friction representing the friction between the layers of powder. The values of pre-shear stresses for Starch were 0.303, 0.600, 1.197, 2.404 and 4.839 kPa, whereas the same for Magnesium Tri-Silicate powders were 0.301, 0.597, 1.194, 2.399 and 4.835 kPa, respectively. The values of major consolidation stress (σ_1) on the powder sample and unconfined yield strength (σ_c) of the powder were obtained from the yield locus. The plot between σ_1 and σ_c. is known as the flow function curve. Figure 4.3.2 shows the flow function curves for Starch and Magnesium Tri-Silicate. The flow function curve can be divided in four parts based on Jenike's flowability classification (Schulze, 2008). Flow Index (FI) is defined as the reciprocal of the flow function curve slope (σ_1/σ_c) and this represents the relative flowability of the powders. Typical values of Flow Index (FI) and the slope of flow function curve for Magnesium Tri-Silicate at a pre-shear value of 1.197 kPa were 1.9624 and 0.30, respectively. Values of the same parameters under the same pre-shear values for Starch were 2.3867 and 0.22, respectively. Figure 4.3.2 shows that the flow function curves for both the powders are almost superimposing on each other. At low stress values, both the powders are cohesive and with an increase in the value of consolidation stress, both the powders have become easy flowing almost at the same point. Based on the results of flow function curves, both powders were found to be equally "cohesive" and equally "easy flowing" (depending on the major principal consolidation stress).

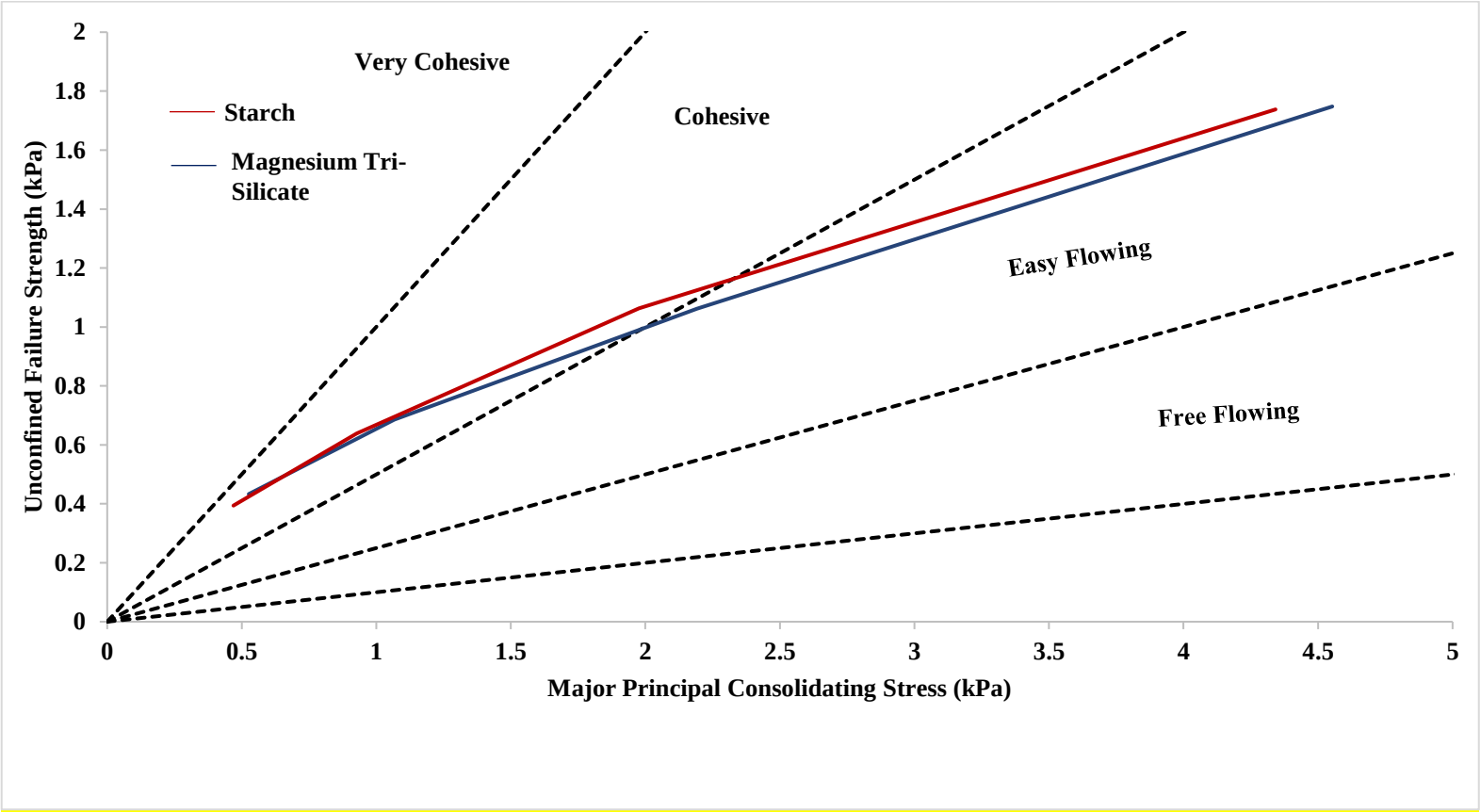

Figure 4.3.2: Flow function curves for Starch and Magnesium Tri-Silicate powders based on instantaneous flow function test results

Effective angle of internal friction (δ) represents the ratio of major to minor consolidation stresses over the powder element under steady flow condition (Jenike, 1964). The variation of effective angle of internal friction with major consolidation stress is shown in Figure 4.3.3.

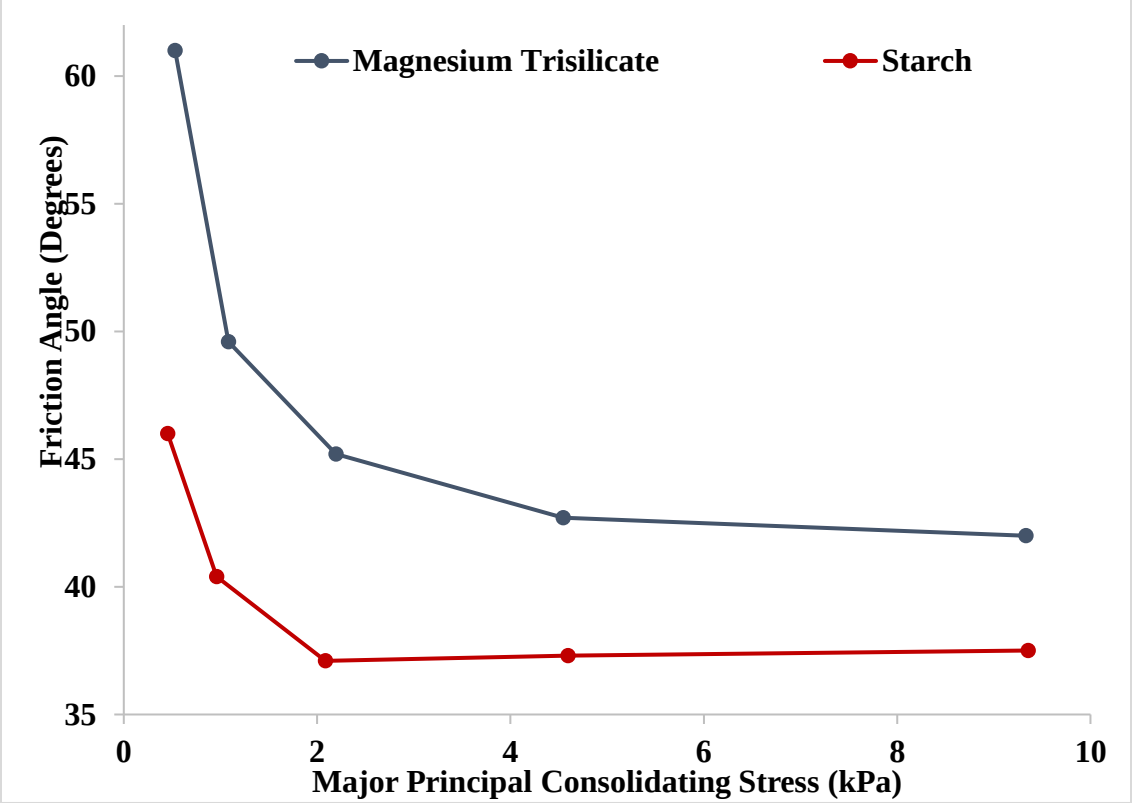

Figure 4.3.3: Effective angle of internal friction versus major consolidation stress for Starch and Magnesium Tri-Silicate samples

The effective angle of internal friction represents the relative contribution of the adhesive forces to the frictional forces. Figure 4.3.3 shows that the effective angle of internal friction values increase at lower consolidation stresses for both Magnesium Tri-Silicate and Starch, indicating that both the powders are of cohesive nature (Schulze, 2008). It can be seen that the trends become

almost flat at higher consolidation stresses. The reason for this decreasing trend is that although both the forces of particle to particle friction and adhesion increase simultaneously with an increase in consolidation stress (consolidation results in particles to come closer to each other), but the increase of frictional forces between the particles caused due to enhanced surface to surface friction and interlocking is stronger than the increase in adhesive forces (due to Van der Waals effect) (Schulze, 2008). Table 4.3.2 provides different states of stress conditions (some typical values) of instantaneous flow property testing.

Table 4.3.2: Sample test data for flow property testing for Magnesium Tri-Silicate and Starch Samples

Consolidation endpoint (kPa)	**Major principal consolidating stress (kPa)**	**Unconfined failure strength (kPa)**	**Gradient**	**Angle (°)**	**Cohesion (kPa)**	**Effective angle of internal friction (°)**
Magnesium Tri-Silicate						
0.301	0.531	0.458	0.37	20.2	0.16	61
0.597	1.081	0.712	0.48	25.6	0.225	49.6
1.194	2.194	1.118	0.55	29	0.329	45.2
2.399	4.546	1.823	0.6	31	0.516	42.7
4.835	9.331	3.177	0.64	32.5	0.871	42
Starch						
0.303	0.454	0.309	0.34	18.8	0.111	46
0.6	0.961	0.522	0.39	21.3	0.178	40.4
1.197	2.086	0.874	0.44	23.7	0.285	37.1
2.404	4.595	1.352	0.55	28.9	0.399	37.3
4.839	9.356	2.364	0.59	30.6	0.674	37.5

Wall friction and bulk density tests

Figure 4.3.4 shows the trends of wall friction angles versus normal stress for Starch and Magnesium Tri-Silicate powders. Wall friction angle (φ_w) represents the friction between wall material and the powder layer adjacent to the walls at a given normal stress.

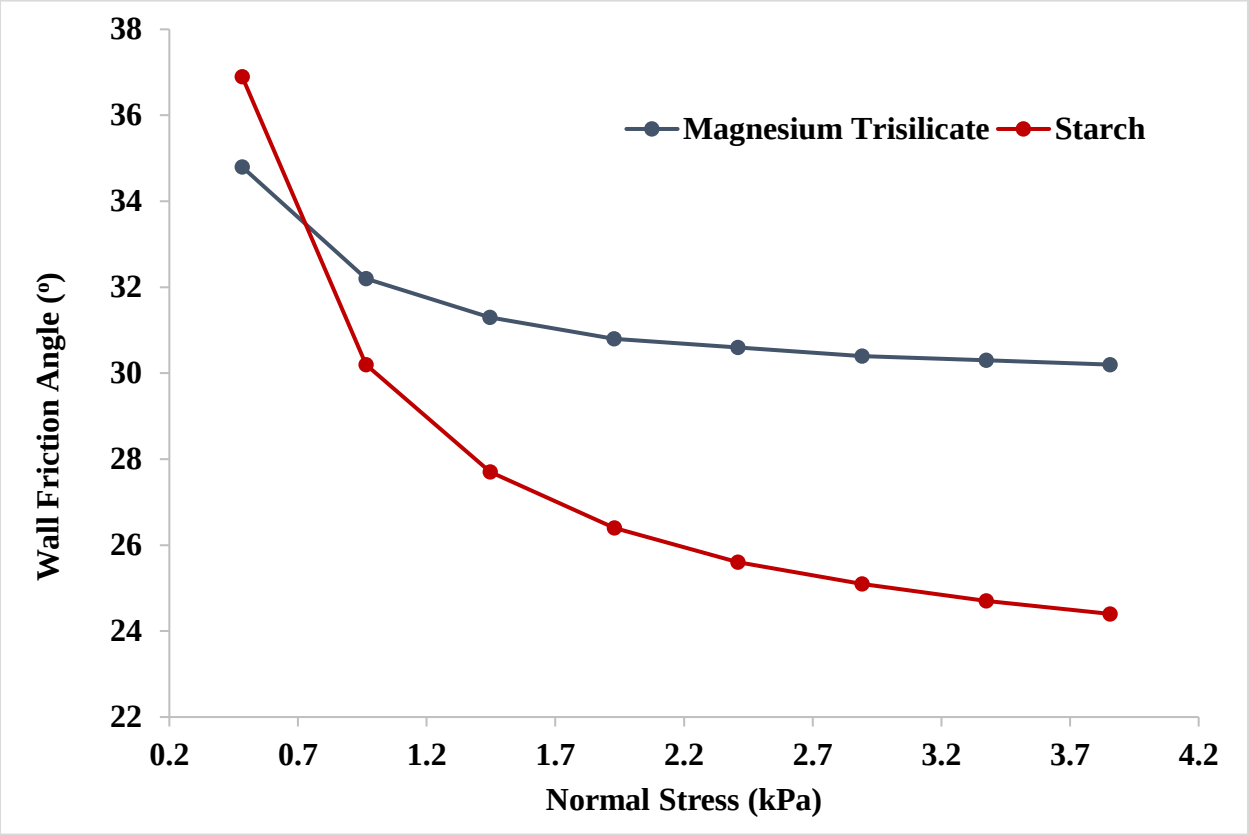

Figure 4.3.4: Trends of wall friction angle versus major consolidation stress for Starch and Magnesium Tri-Silicate powders

It can be seen that at lower normal stress values, both the powders exhibit high (and similar) wall friction angle values. The wall friction angle values get reduced with an increase in the value of normal stress for both the powders, with Magnesium Tri Silicate generally providing higher wall

friction angles compared to starch. Figure 4.3.5 shows the variation of bulk density with an increase in normal stress for Starch and Magnesium Tri-Silicate powders.

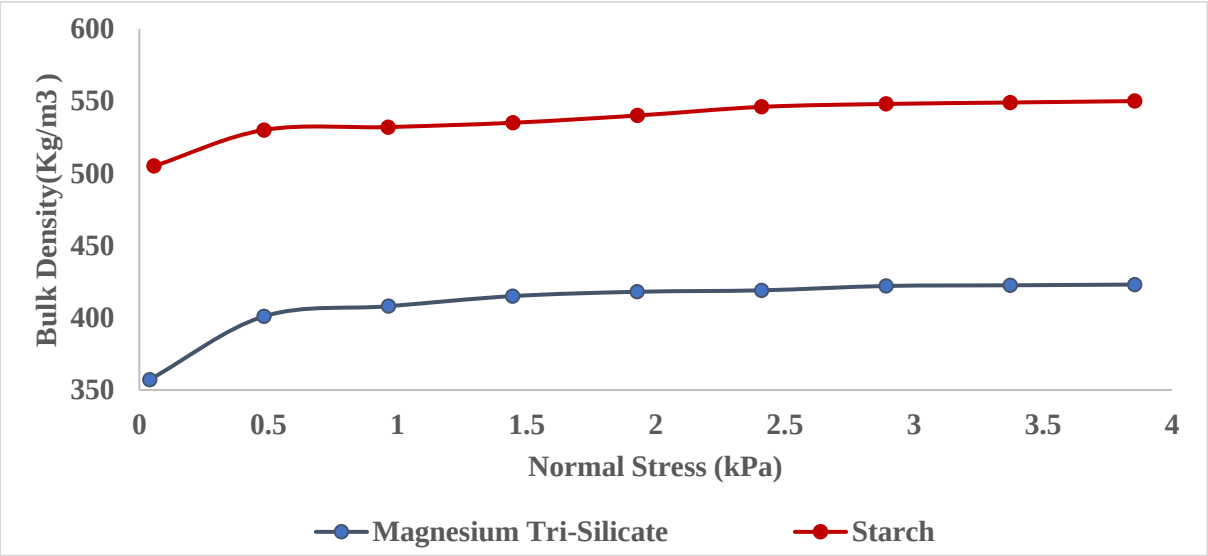

Figure 4.3.5: Bulk density versus normal stress for Starch and Magnesium Tri-Silicate powders

Figure 4.3.5 shows that the trends of bulk density versus normal stress for both the powders follow a sharp rising curve at low stress. Following this, the curves tend to get flatten out towards the higher stress values. The reduction of slope at higher normal stress is caused due to the gradual loss of air gaps or voids within the particles (i.e. gradual loss of porosity with the applied load).

Time consolidation tests

Bulk solids tend to gain additional strength if stored at rest under compressive stress for a long-time of period. This effect is known as time consolidation (Schulze, 2008) and it can be experienced when the powders stored overnight or over the weekend or during the shutdown condition in a plant (typically can occur in a pharmaceutical plant). Gain in strength due to time consolidation is caused by visco-plastic or plastic deformation at particle contacts, which would lead to an enhancement of the acting adhesive forces (as a result of reduction of distance between the particles and enlargement of contact areas). The other possible cause of time consolidation could be due to the formation of solid bridges due to solid crystallizing when drying moist bulk solids (Schulze, 2008). For the time consolidation tests, the powders were subjected to static load (i.e. it was not sheared) for a time span is 12 hours. This time period was chosen as generally these powders (Magnesium Tri-Silicate and Starch) are stored overnight in plants. Table 4.3.3 and 4.3.4 compare the unconfined yield stress for Magnesium Tri-Silicate and Starch powders before and after time consolidation for different pre-shear conditions.

Table 4.3.3: Unconfined yield strength for Magnesium Tri-Silicate powder before and after time consolidation

Sample	**σ_c at σ_{pre1} kPa**	**σ_c at σ_{pre2} kPa**	**σ_c at σ_{pre3} kPa**	**σ_c at σ_{pre4} kPa**
Magnesium Tri-Silicate (before time consolidation test)	0.433	0.686	1.062	1.748
Magnesium Tri-Silicate (after time consolidation test)	0.475	0.749`	1.167	1.967

Table 4.3.4: Unconfined yield strength for Starch powder before and after time consolidation

Sample	**σ_c at σ_{pre1} kPa**	**σ_c at σ_{pre2} kPa**	**σ_c at σ_{pre3} kPa**	**σ_c at σ_{pre4} kPa**
Starch (before time consolidation test)	0.394	0.639	1.063	1.738
Starch (after time consolidation test)	0.476	0.786`	1.258	2.241

Table 4.3.3 and 4.3.4 show that both the powders have gained strength (increase in unconfined yield stress) after time consolidation (by comparing the unconfined yield strength values before and after time consolidation). Figure 4.3.6 shows the flow function curves for Magnesium Tri-

Silicate after time consolidation. It can be seen that while the Magnesium Tri-Silicate powders continue to remain in the “cohesive” and “easy flowing” regime, the Starch have shifted its position entirely into the “cohesive region”. It should be also noted that as per Figure 4.3.2, Magnesium Tri-Silicate was shifting from “cohesive” to “easy flowing” regime at a major principal consolidation stress of 2.2 kPa; the same after time consolidation has been increased to about 2.7 kPa. This indicates that the overall cohesiveness nature of Magnesium Tri-Silicate has also increased due to time consolidation.

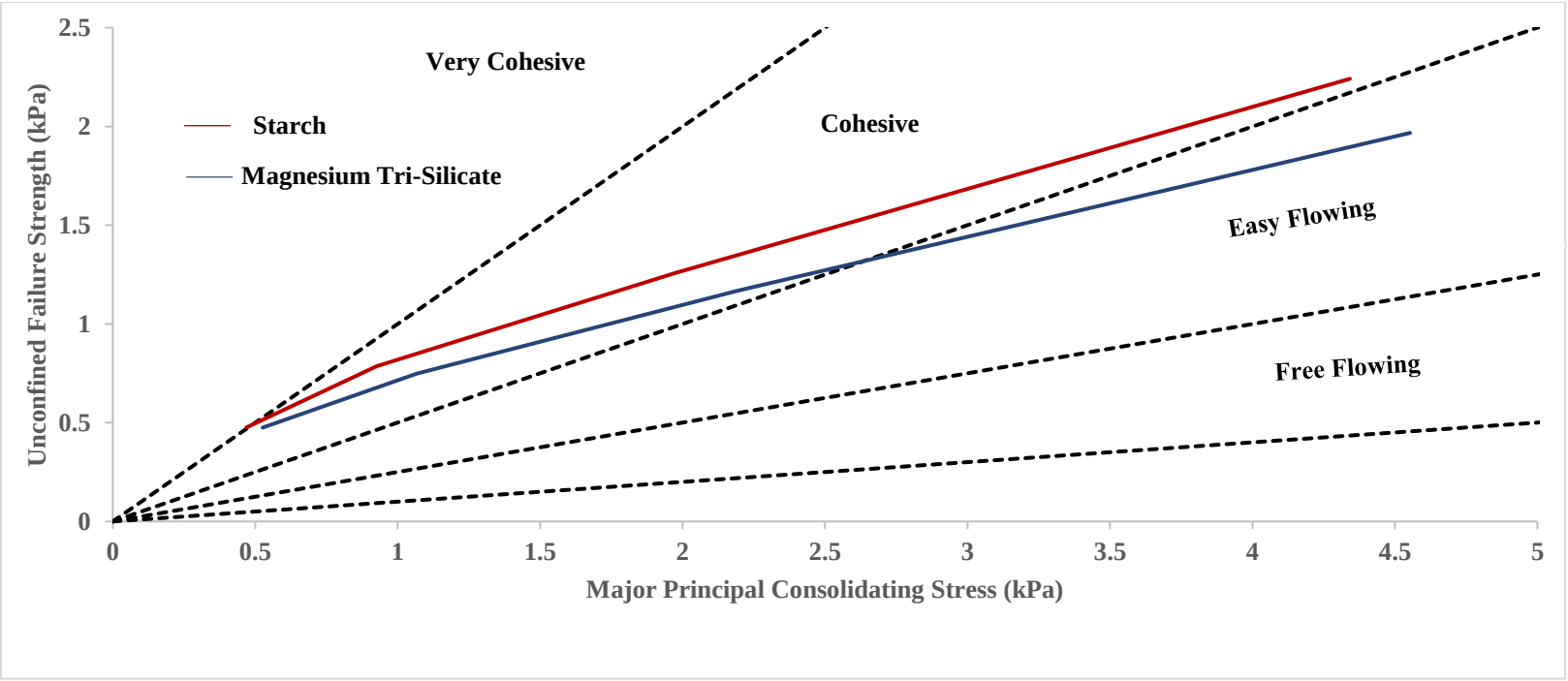

Figure 4.3.6: Flow function curves for Starch and Magnesium Tri-Silicate powders based on time consolidation test results

Critical dimensions of mass flow hopper

Hopper half angle (θ) and outlet opening (D) are important parameters for hopper design for ensuring mass flow of the bulk solids is achieved. Jenike performed pioneering work in this field by mathematically relating between hopper critical dimensions and the powder flow properties. Hopper half angles and critical outlet openings were estimated using equations (4.3.5) and (4.3.6) with the knowledge of powder flow properties found at different pre-shear stresses and wall friction characteristics for both the powders. Using the results obtained from flow property and wall friction tests, the results are shown in Figure 4.3.7.

$$D = \frac{2\ X\ \sigma_c\ X\ 1000}{\rho_b\ X\ g} \tag{4.3.5}$$

$$\theta = \left[90 - \frac{1}{2}\cos^{-1}\left(\frac{1-\sin\delta}{2\sin\delta}\right)\right] - \frac{1}{2}\left[\varphi_w + \sin^{-1}\left(\frac{\sin\varphi_w}{\sin\delta}\right)\right] \tag{4.3.6}$$

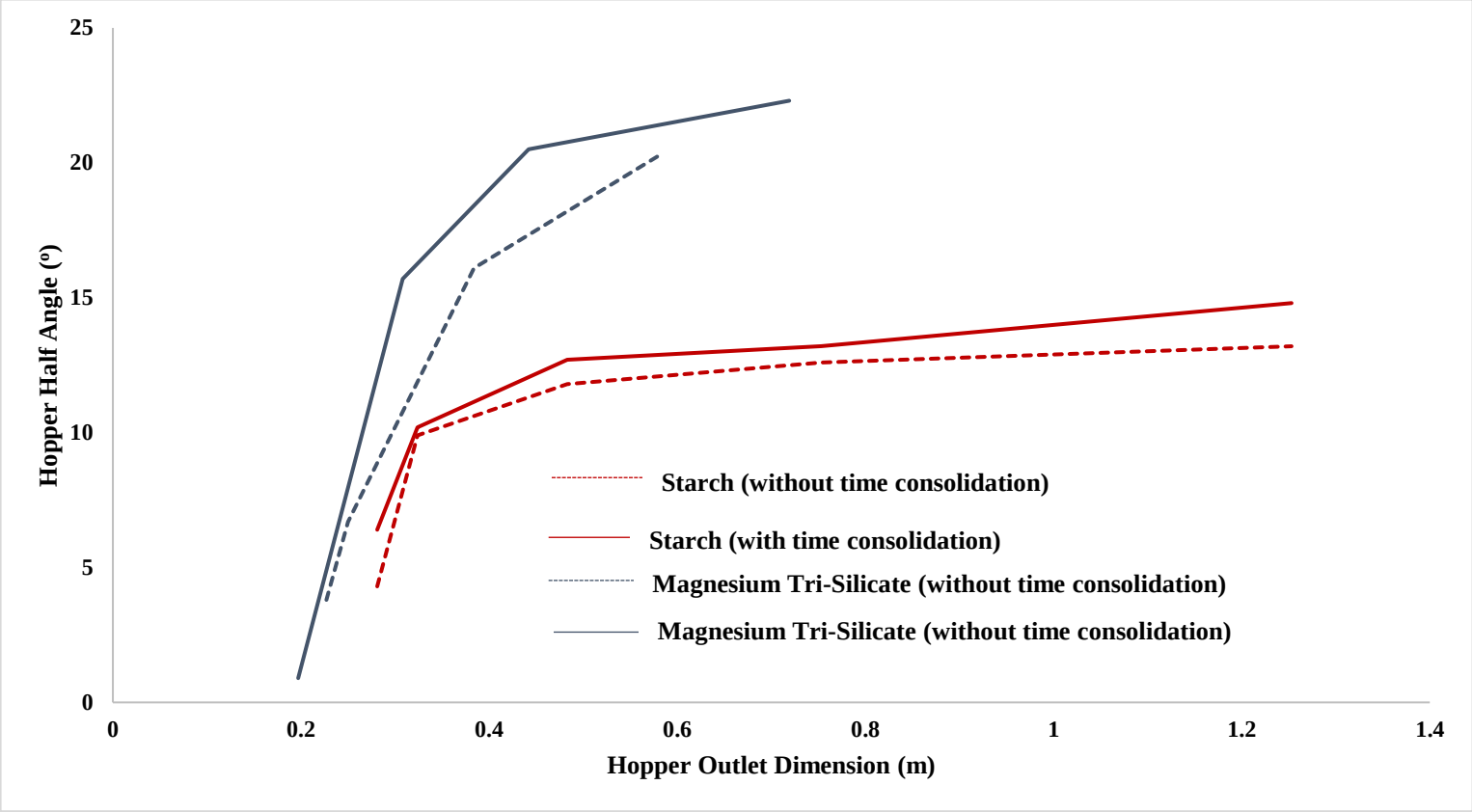

Figure 4.3.7: Comparison of hopper half angle to outlet dimension for Magnesium Tri-Silicate and Starch powders with and without time consolidation effects

Figure 4.3.7 shows that Starch being more cohesive would require larger hopper outlet dimension (for the same hopper half angle) than Magnesium Tri-Silicate. While, an increase in hopper half angle is required for Magnesium Tri-Silicate, the plots for Starch are almost superimposing on each other indicating that overnight storage is expected to alter the flow properties of Magnesium Tri-Silicate appreciably (but no such changes are expected for Starch for a 12-hr. period). Overall, the results show that Starch would require additional hopper outlet opening compared to Magnesium Tri-Silicate (under both with and without time consolidation effects) indicating that for these powders, the effect of particle shape and nature of powder surface is more dominant over the effect of having extra fineness in size.

4.4 Results and discussion for Detergent powder sample

4.4.1 Physical properties of powders

Table 4.4.1 provides the various physical properties of detergent powder. Figure 4.4.1 shows the Scanning Electron Microscopy (SEM) images of the powder at the magnification of 450 and 1500. The SEM images provided in Figure 4.4.1 shows that the detergent powders were having relatively more uniform and smooth shapes. Though not exactly spherical, but the lactose powders seem to have less ratio of length to width and hence, closer to having a spherical shape. The more the structure is irregular/needle type (away from spherical), the more is the resistance of the powders to flow under disturbance (such as tapping) or under compressive load. This is due to the fact that the spherical or closer to spherical shaped particles with smooth surface would move against each other more easily compared to irregular or needle shape particles, where the particles would

experience greater frictional resistance to flow pass each other due to larger surface roughness. The detergent particles being coarse and having near spherical shape, are likely to be good candidate for easy flow. Span was determined using equation 4.4.1 to evaluate the range of size distribution.

$$\text{Span} = (d_{90}-d_{10})/d_{50} \quad (4.4.1)$$

Where, d_{50} is defined as the diameter below which half of the powder population lies. Similarly, 10 and 90% of the distribution lies below the size values of d_{10} and d_{90}, respectively.

Porosity (Li et al, 2016) and compressibility index (Ji et al, 2017) were calculated using the following formulae:

$$\text{Porosity} = 1- (\rho_{lb}/\rho_p) \quad (4.4.2)$$

$$\text{Compressibility Index} = 100 \times [1- (\rho_{lb}/\rho_t)] \quad (4.4.3)$$

Table 4.4.1: Physical properties of Detergent

Powders	**d_{10} (µm)**	**d_{50} (µm)**	**d_{90} (µm)**	**ρ_{lb} (kg/m^3)**	**ρ_p (kg/m^3)**	**ρ_t (kg/m^3)**	**Hausner Ratio (HR)**	**CI**	**Porosity**	**Span**	**SSA (m^2/kg)**
Detergent	173	430	685	1157	3238	1435	1.24	19.37	0.6426	1.906	148

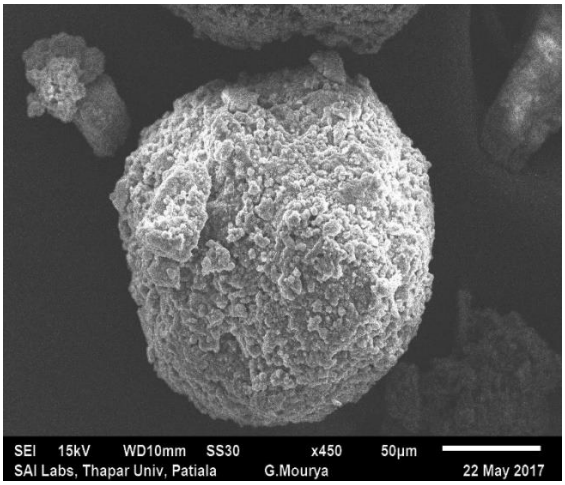

(a) at magnification of 450

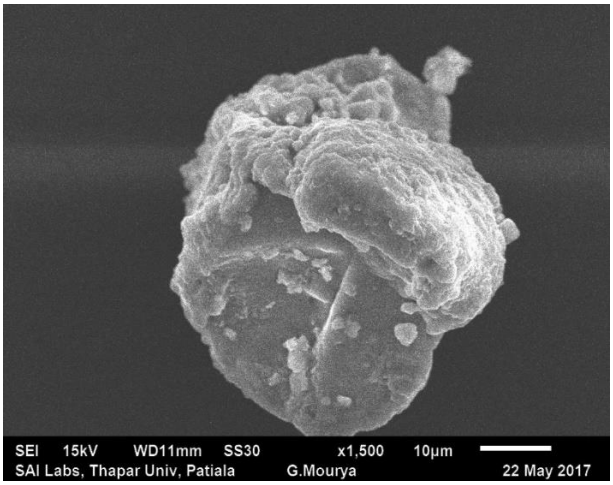

(a) at magnification of 1500

Figure 4.4.1: SEM images of detergent sample

4.4.2 Flow properties of detergent

Yield locus and flow function curves

Yield locus of powders represents the shear stress (τ) necessary to initiate the flow in the powder sample under a given consolidation stress (σ) (Jager et al., 2015). Yield locus is a curve which is generated between normal consolidation stress and shear stress and can be represented by the equation 4.4.4 at any given pre-shear condition.

$$\tau = \sigma \tan \varphi + C \qquad (4.4.4)$$

Where, φ is the internal friction angle representing the magnitude of friction between the layers of powder. The values of pre-shear stresses for powders were 0.318, 0.612, 1.209, 2.413 and 4.850

kPa, respectively. Each yield locus provides major consolidation stress (σ_1) and the corresponding values of unconfined yield strength (σ_c) related to the powder. Figure 4.4.2 shows the flow function curve (a plot between σ_1 and σ_c) for detergent powder. The flow function curve (Figure 4.4.2) has been divided in four parts based on Jenike's flowability classification (Jager et al., 2015)., as reported by Saw et al. (2015). Flow Index (FI) is defined as the reciprocal of flow function curve slope (σ_1/σ_c) and indicates the relative flowability of the powders. Typical values of Flow Index (FI) and the slope of flow function curve for the sample at a pre-shear value of 1.2 kPa were 5.062 and 0.13, respectively. Figure 4.4.2 shows that below the major principal consolidation stress of about 7.2 kPa, the powders fell in the "free flowing" regime. However, above this consolidation stress, this powder fell into the "easy flowing" regime. The reason for the powder being more free flowing has been already explained in the previous section. Figure 4.4.2 is based on instantaneous flow function results.

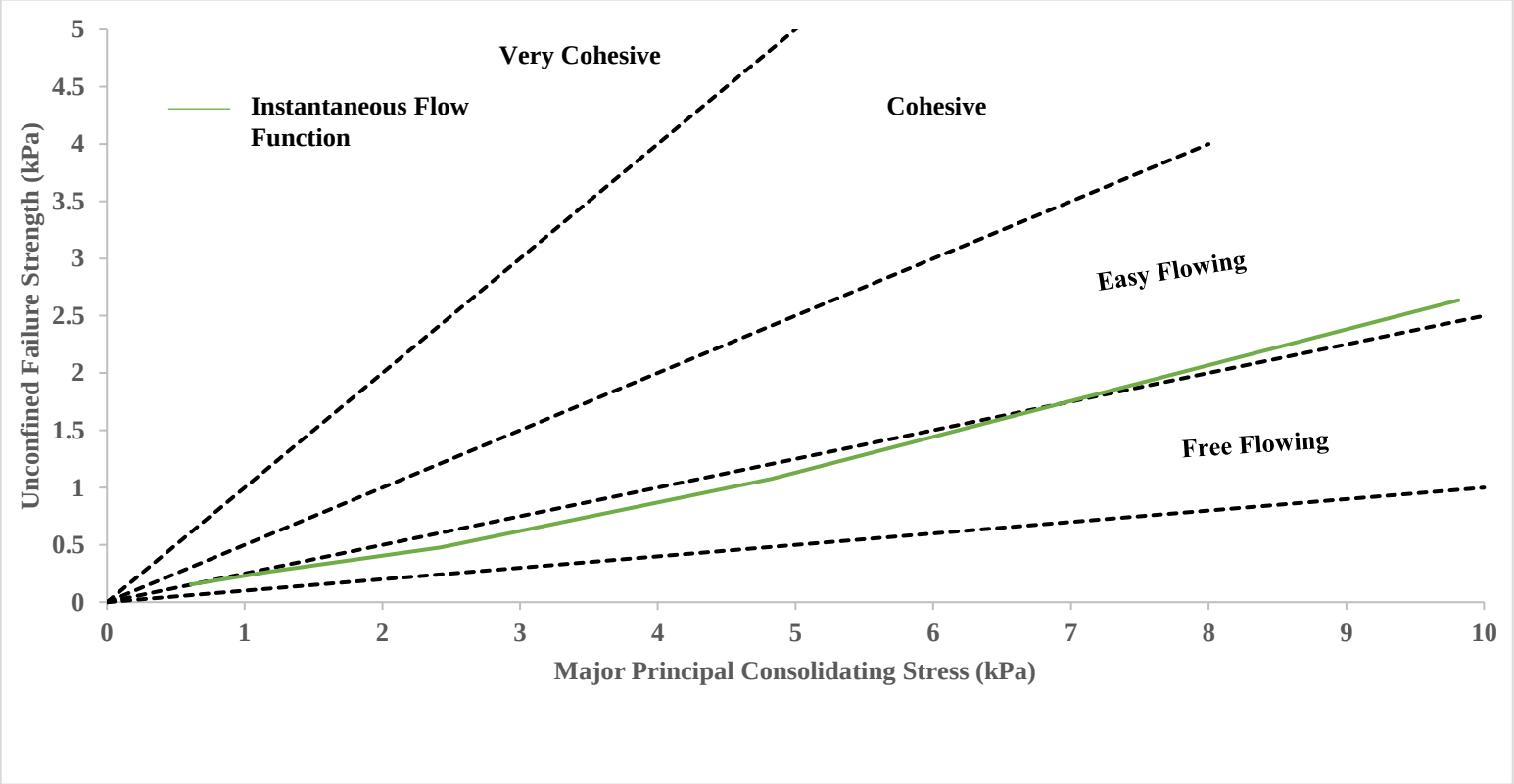

Figure 4.4.2: Flow function curves for detergent without time consolidation

Effective angle of internal friction (δ) is defined as the ratio of major consolidation and minor consolidation stresses over a powder element in steady state flow (Jenike, 1964). The trend of variation of effective angle of internal friction with major consolidation stress is shown in Figure 4.4.3.

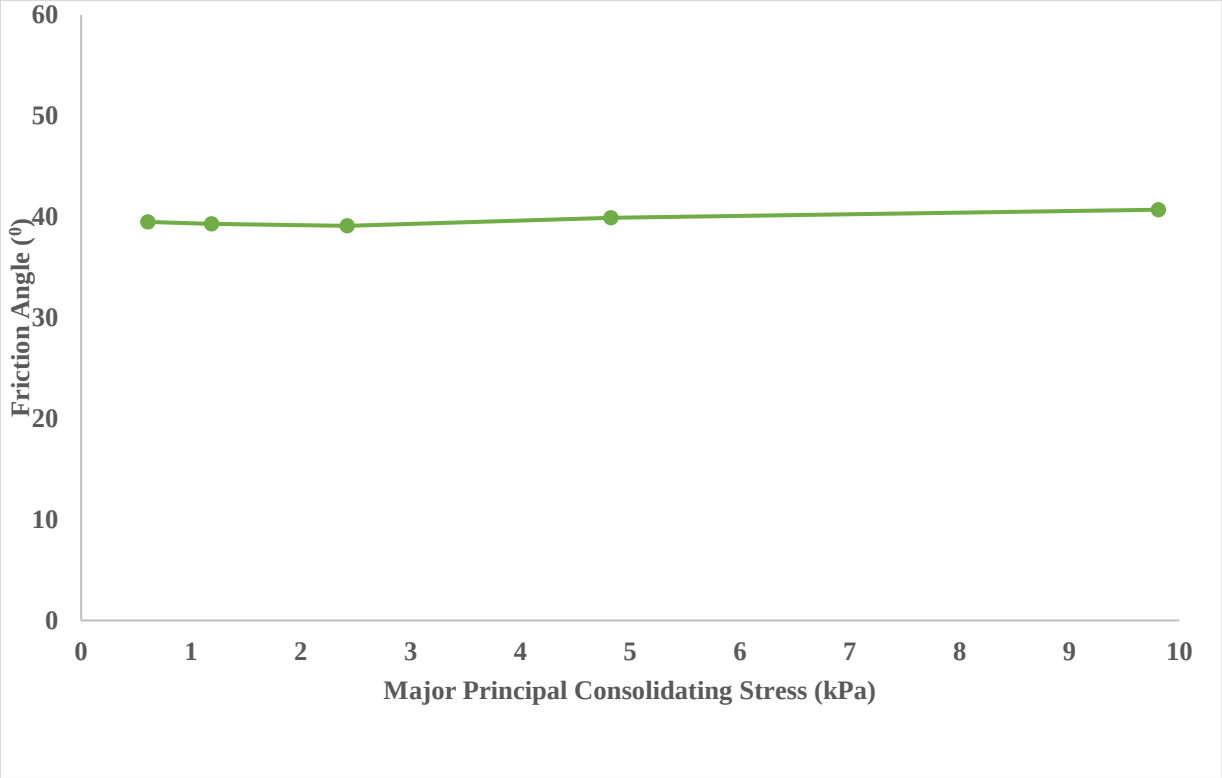

Figure 4.4.3: Effective angle of internal friction versus major consolidation stress for detergent powder

The effective angle of internal friction of powders represents the relative contribution of adhesive forces to frictional forces. Figure 4.4.3 shows that the effective angle of internal friction values is

somehow constant. This indicates that this powder is easy flowing (Schulze, 2008). The reason for the constant nature of the slopes with increasing values of major consolidation stress is that although both the forces of particle to particle friction and adhesion increase simultaneously (as consolidation causes the particles to come closer to each other) with the increase of major consolidation stress, but the increase of frictional forces between the particles caused due to enhanced surface to surface contact friction and interlocking is almost equal to the increase in adhesive forces, such as the Van der Waals effect (Schulze, 2008). As a result of equal prevalence of frictional forces, the effective angle of internal friction is constant across the entire range of major consolidation stresses. Table 4.4.2 provides different states of stress conditions with some typical values of instantaneous flow property testing.

Table 4.4.2: Sample test data for flow property testing for detergent

Consolidation endpoint (kPa)	**Major principal consolidating stress (kPa)**	**Unconfined failure strength (kPa)**	**Gradient**	**Angle (°)**	**Cohesion (kPa)**	**Effective angle of internal friction (°)**
0.318	0.610	0.154	0.64	32.8	0.042	39.5
0.612	1.188	0.267	0.66	33.4	0.072	39.3
1.209	2.425	0.479	0.67	34	0.127	39.1
2.413	4.827	1.077	0.68	34.1	0.286	39.9
4.850	9.814	2.636	0.66	33.6	0.707	40.7

Wall friction and bulk density tests

Figure 4.4.4 shows the trends of wall friction angles versus normal stress for the detergent powder. The friction between wall material and the powder layer adjacent to the walls at a given normal stress is given by wall friction angle (φ_w).

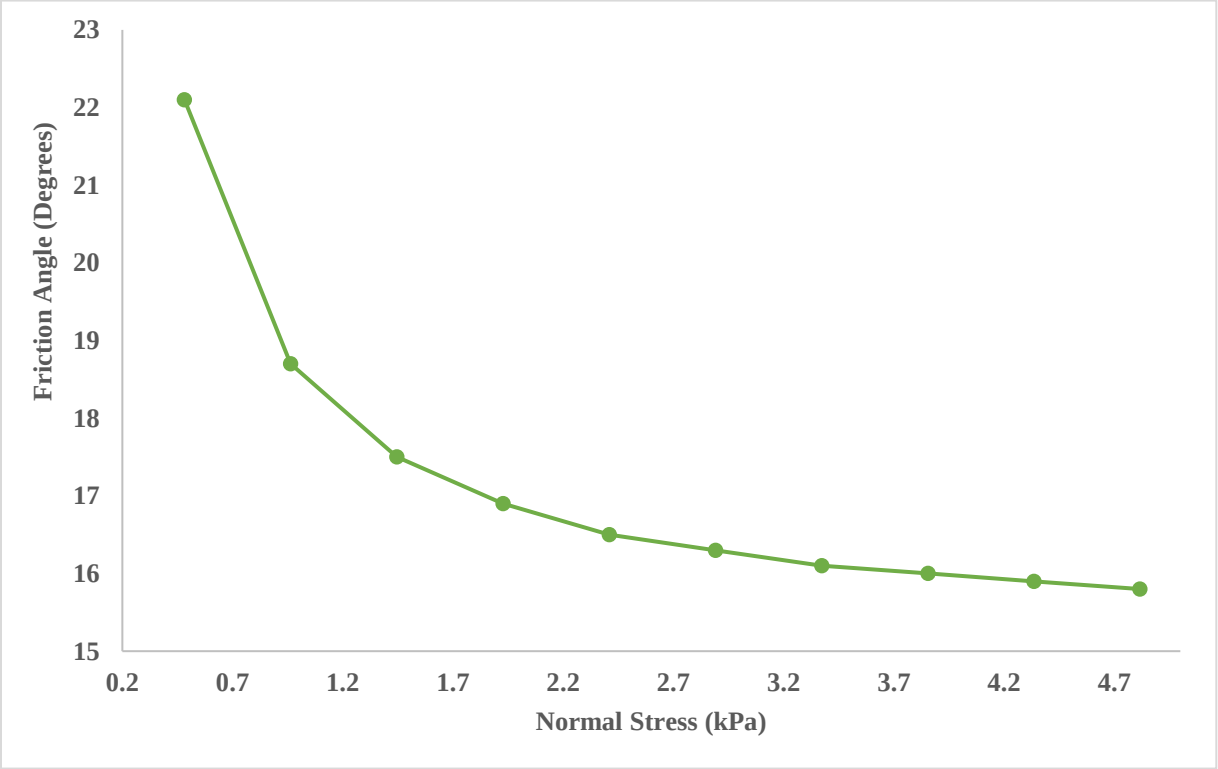

Figure 4.4.4: Trend of wall friction angle versus major consolidation stress for detergent

It can be seen from Figure 4.4.4 that the wall friction angle decreases with an increase in normal stress. Figure 4.4.5 shows the variation of bulk density with an increase in normal stress for the sample. The trends of bulk density versus normal stress for both powder follow a relatively sharper rising curve at low normal stress values. After the initial sharp rise, the curves tend to get flatten out in the higher stress value ranges.

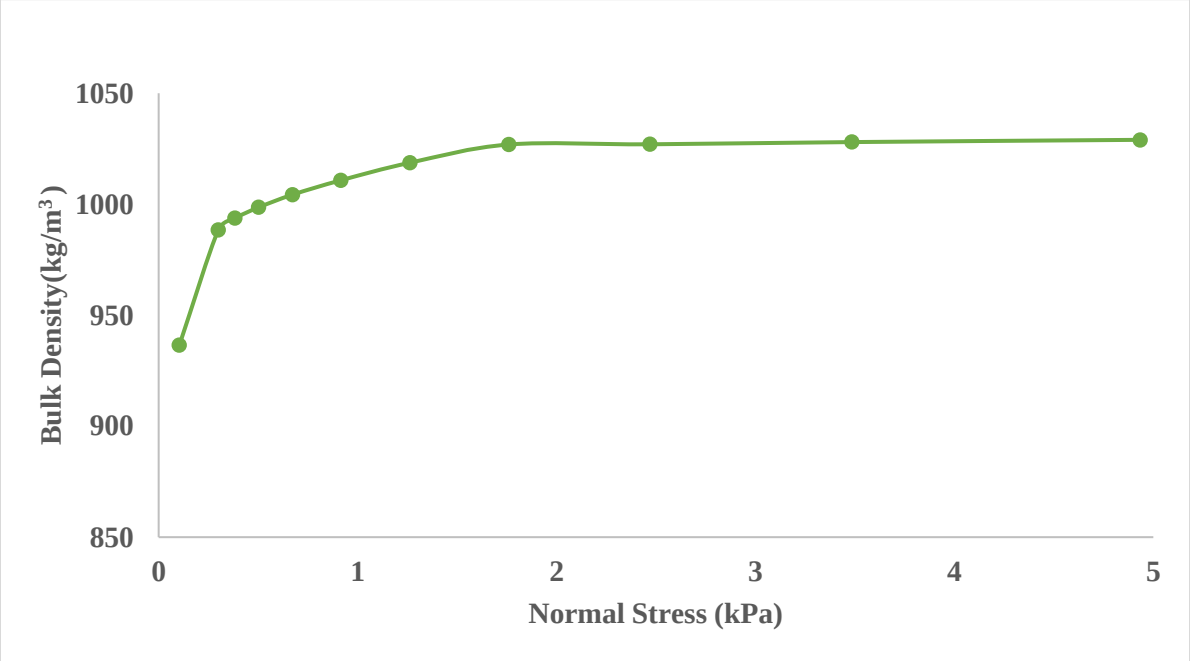

Figure 4.4.5: Bulk density versus normal stress for di-calcium phosphate and calcium sulphate powders

Time consolidation tests

Certain bulk powders gain additional strength when stored at rest under compressive stress for a long-time period. This effect is known as time consolidation (Schulze, 2008). This may happen when the powders are stored overnight or over the weekend or during the shutdown condition in a plant, e.g. in a detergent manufacturing industry. Gain in strength due to time consolidation is contributed by visco-plastic or plastic deformation at particle contact zones, which increases the adhesive forces due to the shortening of distance between the particles and enhancement in contact areas, development of solid bridges due to solid crystallization during the drying of moist bulk

solids etc. (Schulze, 2008). In time consolidation tests, the sample was subjected to a static load, i.e. it was not sheared, for a time span is 12 hours. This time frame was kept as generally these powders (calcium sulphate and dicalcium phosphate) are stored overnight in detergent manufacturing industries. Table 4.4.3 compares the unconfined yield stress for detergent sample before and after time consolidation under different pre-shear stress applications.

Table 4.4.3: Unconfined yield strength for detergent before and after time consolidation

Sample	σ_c at σ_{pre1} kPa	σ_c at σ_{pre2} kPa	σ_c at σ_{pre3} kPa	σ_c at σ_{pre4} kPa	σ_c at σ_{pre5} kPa
Detergent (before time consolidation test)	0.154	0.267	0.479	1.077	2.636
Detergent (after time consolidation test)	0.204	0.478	1.24	2.54	5.478

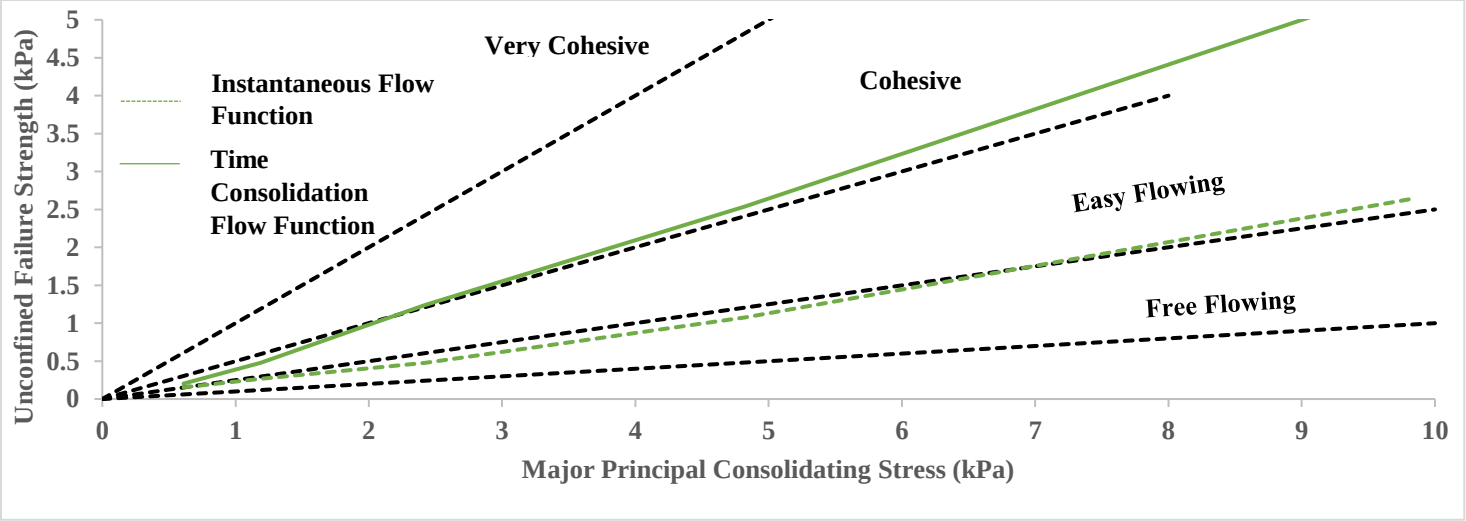

Figure 4.4.6: Flow Function curve with and without time consolidation for the detergent sample

A comparison of unconfined yield strength results before and after time consolidation Table 4.4.3 show that the powder has gained additional strength after time consolidation. Figure 4.4.6 shows the flow function curves for the detergent powder, before and after time consolidation. The results show that the powder has become "cohesive" at low stresses after time consolidation from being "free flowing" before time consolidation.

Critical dimensions of mass flow hopper

Hopper half angle (θ) and outlet opening (D) are the critical parameters for hopper design especially to maintain reliable mass flow of powders. Jenike, A.W., 1964, carried out pioneering work by deriving mathematical relations powder flow properties. Hopper half angles and critical outlet openings were determined from equations (4.4.5) and (4.4.6) by using the results obtained from flow property and wall friction tests (corresponding to instantaneous and time consolidation tests). The results are shown in Figure 4.4.7.

$$D = \frac{2\ X\ \sigma_c\ X\ 1000}{\rho_b\ X\ g} \tag{4.4.5}$$

$$\theta = \left[90 - \frac{1}{2}\cos^{-1}\left(\frac{1-\sin\delta}{2\sin\delta}\right)\right] - \frac{1}{2}\left[\varphi_w + \sin^{-1}\left(\frac{\sin\varphi_w}{\sin\delta}\right)\right] \tag{4.4.6}$$

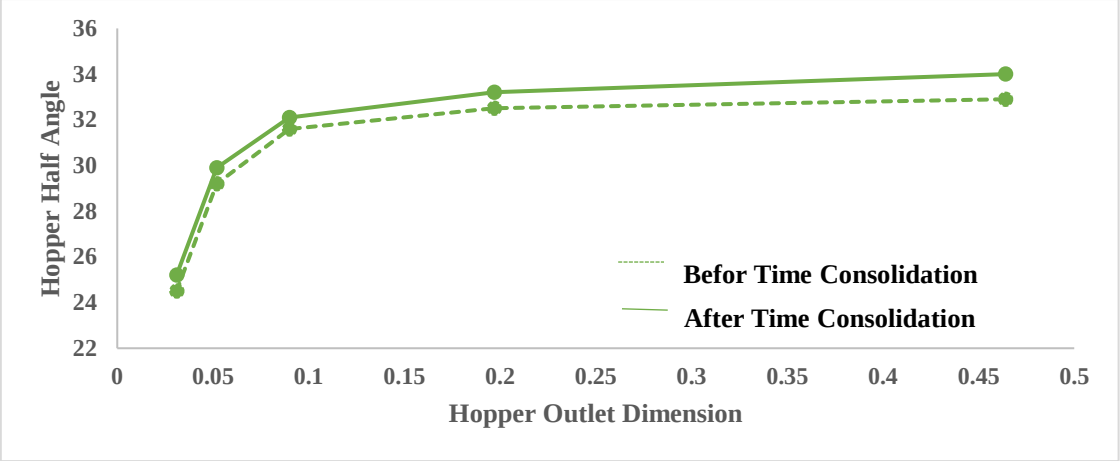

Figure 4.4.7: Comparison of hopper half angle to outlet dimension for detergent with and without time consolidation effects

Figure 4.4.7 shows that for this powder, a considerable amount of additional hopper outlet size is required (for the same hopper angle) after time consolidation compared to the requirement outlet openings obtained from instantaneous test results.

Chapter-5

Conclusion and Future Scope

5.1 Conclusions

The paracetamol powders were found to be more cohesive than the lactose powders due to smaller particle size, larger specific surface area and irregular surface profile. This has been confirmed by the lower loose poured bulk density, larger porosity and larger tapped density for the paracetamol powders. Paracetamol powder being relatively more cohesive require wider hopper outlet dimensions than the lactose powders with and without time consolidation. Time consolidation has been found to have a stronger effect on paracetamol (than lactose), requiring a considerably a larger hopper outlet dimension (for the same hopper angle). The results clearly indicate that a good hopper design should be based on specific product behavior. The hopper that may allow lactose to flow easily (maintaining mass flow condition), can create arching for paracetamol. Also, time consolidation test plays a vital role in determining the flow properties of powders that are stored (e.g. overnight) before being handled. The powders may change their flow properties from being easy flowing to cohesive to very cohesive over time and could create severe flow problems (inadequate or chocked flow).

The di-calcium phosphate powders were found to be more cohesive than the calcium sulphate powders as indicated by larger porosity and larger tapped density of the di-calcium phosphate powders. Di-calcium phosphate powder being relatively more cohesive require wider hopper outlet dimensions than the calcium sulphate powders without time consolidation. Time

consolidation has been found to have a stronger effect on calcium sulphate, requiring a considerably a larger hopper outlet dimension (for the same hopper angle) after time consolidation. The results clearly indicate that a reliable hopper design should be based on specific powder property data. The hopper that may allow calcium sulphate to flow easily (maintaining mass flow condition), can create arching for di-calcium phosphate.

While the Starch powders were found to contain more fines (that would tend to cause Starch more cohesive), in contrast, the Magnesium Tri-Silicate powders were found to be characterized by having more irregular shapes (which tends to resist powder flow). Due to the limited interference that could be drawn from the physical property tests (characterization tests), flow property test results were relied upon as confirmatory tests. The instantaneous flow function results have shown that both the powders remain in “cohesive” to “easy flowing” range (having almost superimposed flow function curves). However, after time consolidation, Starch has entered completely into the “cohesive” regime (within the applied stress limits), while the Magnesium Tri-Silicate powders continue to remain in the “cohesive” to “easy flowing” regime (with more portion shifted to “cohesive” regime). Overall, the results show that Starch would require additional hopper outlet opening compared to Magnesium Tri-Silicate (under both with and without time consolidation effects). This indicates that for these powders, the effect of particle shape and nature of powder surface is more dominant over the effect of having extra fineness in size. Starch showed appreciable gain in strength due to time consolidation, whereas no such effect was apparent for Magnesium Tri-Silicate for the given 12 hr period.

Time consolidation has been found to have a stronger effect on the detergent sample, requiring a considerably a larger hopper outlet dimension (for the same hopper angle) after time

consolidation. The results clearly indicate that a reliable hopper design should be based on specific powder property data. Time consolidation test plays a major role in designing storage facilities of powders that are stored overnight. The powders may change their flow properties from being easy/free flowing to cohesive over time and could potentially result in severe flow problems (such as arching). Models for cohesion and unconfined yield stress have been developed using particle size distribution data, compressibility index and pre-shear stress condition (see Appendix A).

For a good design, the engineer is recommended to carry out necessary flow property testing with and without time consolidation effects into consideration for designing practical storage or feeding systems to achieve desirable mass flow condition.

5.2 Future scope of work

- Large scale shear cell tester can be developed for better understanding of the flowability of the powders at high consolidation stresses.
- There is a need to carry out further studies on the effect of time consolidation in the powder flowability.
- There is a need to fundamentally study the physico-chemical changes occurring at the particle-particle-wall interface under time consolidation condition.

References

Abdullah, E.C. and Geldart, D., 1999. The use of bulk density measurements as flowability indicators. Powder Technology, 102(2),151-165.

Amagliani, L., O'Regan, J., Kelly, A.L. and O'Mahony, J.A., 2016. Physical and flow properties of rice protein powders. Journal of Food Engineering, 190, 1-9.

Bian, Q., Sittipod, S., Garg, A. and Ambrose, R.K., 2015. Bulk flow properties of hard and soft wheat flours. Journal of Cereal Science, 63, 88-94.

Dudhat, S.M., Kettler, C.N. and Dave, R.H., 2016. To Study Capping or Lamination Tendency of Tablets Through Evaluation of Powder Rheological Properties and Tablet Mechanical Properties of Directly Compressible Blends. AAPS PharmSciTech, 1-13.

Fitzpatrick, J.J., Barringer, S.A. and Iqbal, T., 2004. Flow property measurement of food powders and sensitivity of Jenike's hopper design methodology to the measured values. Journal of Food Engineering, 61(3), 399-405.

Freeman, R. (2007). Measuring the flow properties of consolidated, conditioned and aerated powders- A comparative study using powder rheometer and a rotational shear cell. Powder Technology. 174:25-33.

Ganeshan, V., Rosentrter, K.A and Muthukumarappan, K. (2008).Flowablity and handling characteristics of bulk solids and powders- a review with implications for DDGS. Bio systems Engineering. 101: 425-435.

Geldart, D., Abdullah, E.C., Verlinden, A. (2009). Characterization of dry powders. Powder Technology. 190: 70-74.

Hart, Abarasi., 2015. Effect of Particle Size on Detergent Powders Flowability and Tabletability. Journal of Chemical Engineering and Process Technology, (Vol.6),1-4.

Ittershagen, T., Schwedes, J., Kwade, A. (2011). A new powder tester to investigate the anisotropic consolidation behaviour. Powder Technology: 85-89.

Ittershagen, Thomas, Zetezener, Herald. Schwedes, Jorg., Kwade, Arno. Anisotropic behaviour of bulk solids and its effect on silo design. Powder technology 247 (2013): 260-264.

Jager, P.D., Bramante, T. and Luner, P.E., 2015. Assessment of Pharmaceutical Powder Flowability using Shear Cell-Based Methods and Application of Jenike's Methodology. Journal of pharmaceutical sciences, 104(11),3804-3813.

Jaggi, V., Leaper, M.C. and Ingham, A., 2016. Measuring the flow properties of small powder samples using an avalanche tester. Drying Technology, 34(6), 723-728

Jan, S., Jan, K. and Saxena, D.C., 2016, January. Flow property measurement of rice flour-A Review. In MATEC Web of Conferences (Vol. 57). EDP Sciences.

Jenike, A.W., 1964. Storage and flow of solids, bulletin no. 123. Bulletin of the University of Utah, 53,26.

Ji, J., Fitzpatrick, J., Cronin, K., Fenelon, M.A. and Miao, S., 2017. The effects of fluidised bed and high shear mixer granulation processes on water adsorption and flow properties of milk protein isolate powder. Journal of Food Engineering, 192,19-27.

Leturia, M., Benali, M.Lagarde, S., Ronga, I.and Saleh, K. Characterization of flow properties of cohesive powders: A comparative study of traditional and new methods. Powder technology 253 (2014):406-423.

Leung, L.Y., Mao, C., Chen, L.P. and Yang, C.Y., 2016. Precision of pharmaceutical powder flow measurement using ring shear tester: High variability is inherent to powders with low cohesion. Powder Technology, 301, 920-926.

Li, R., Roos, Y.H. and Miao, S., 2016. Influence of pre-crystallisation and water plasticization on flow properties of calcium sulphate/WPI solids systems. Powder Technology, 294, 365-372.

Maarup, Claus, Hjuler, Klaus. Dam-Johnsen, Kim. High temperature cement raw meal flowablity. Powder technology (2014): 686-690.

Morin, G. and Briens, L., 2013. The effect of lubricants on powder flowability for pharmaceutical application. AAPS PharmSciTech, 14(3), 1158-1168.

Opaliński, I., Chutkowski, M. and Hassanpour, A., 2016. Rheology of moist food powders as affected by moisture content. Powder Technology, 294, 315-322.

Pingali, K.C., Chatarla, S.K., Tracy, B.A. and Byrnes, B.A., 2016. Sensing Electrostatic Charge Generation During Granular Flow of Pharmaceutical Powders in a Flow Tester. Journal of Pharmaceutical Innovation, 1-10.

Ripp, M., Debele, Z.A. and Ripperger, S., 2015. Determination of Bulk Flow Property of tef Flour and Seed and Design of a Silo. Particulate Science and Technology, 33(5), 494-502.

Saw, H.Y., Davies, C.E., Paterson, A.H. and Jones, J.R., 2015. Correlation between powder flow properties measured by shear testing and Hausner ratio. Procedia Engineering, 102, 218-225.

Schulze, D., 2008. Powders and bulk solids. Behaviour, Characterization, Storage and Flow. Springer.

Slettengren, K., Xanthakis, E., Ahrné, L. and Windhab, E.J., 2016. Flow Properties of Spices Measured with Powder Flow Tester and Ring Shear Tester-XS. International Journal of Food Properties, 19(7), 1475-1482.

Sun, C.C., 2016. Quantifying effects of moisture content on flow properties of microcrystalline cellulose using a ring shear tester. Powder Technology, 289, 104-108.

Teunou, E., Fitzpatrick, J.J. and Synnott, E.C. (1999). Characterization of food powder flowablity. Journal of Food Engineering. 39: 31-37.

Trementozzi, A.N., Leung, C.Y., Osei-Yeboah, F., Irdam, E., Lin, Y., MacPhee, J.M., Boulas, P., Karki, S.B. and Zawaneh, P.N., 2017. Engineered particles demonstrate improved flow properties at elevated drug loadings for direct compression manufacturing. International journal of pharmaceutics, 523(1), 133-141.

Wang, Y., Koynov, S., Glasser, B.J. and Muzzio, F.J., 2016. A method to analyze shear cell data of powders measured under different initial consolidation stresses. Powder Technology, 294, 105-112.

Wang, Y., Snee, R.D., Meng, W. and Muzzio, F.J., 2016. Predicting flow behavior of pharmaceutical blends using shear cell methodology: A quality by design approach. Powder Technology, 294, 22-29.

Zigan , S., Thrope, R.B., Tuzun, U., Enstad, G.G., Battistin, F. (2008) . Theoretical and experimental testing of a scale rule for air current segregation of alumina powder in cylindrical silos. Powder Technology 183: 133-145.

Appendix A

Modeling Cohesion and Unconfined Yield Stress

A new model has been developed to study the effect of physical properties on cohesion and unconfined yield strength. We can obtain the values of cohesion and unconfined yield stress within five pre-shear stresses. In the model, cohesion has been taken as a function of adequate particle size, compressibility index and pre-shear stress. Selective determination of correlation coefficients shows the CI and σ_{pre} have higher influence on cohesion and unconfined yield stress followed by the effective particle size. This indicates that the flowability of the powder depends more on CI and σ_{pre} as compared to effective particle size. Cohesion model for the pharmaceutical powders is given by: -

$$C = 0.00125\ (d_{50}/S)^{0.092302}(CI)^{1.664458}\left(\sigma_{pre}\right)^{0.6516} \qquad [r^2 = 0.925]$$

Unconfined yield stress model for the pharmaceutical powders is given by: -

$$\sigma_c = 0.01409(d_{50}/S)^{0.090844}(CI)^{1.276733}\left(\sigma_{pre}\right)^{0.7074} \qquad [r^2 = 0.93]$$

The comparison of the modeled cohesion values and the cohesion values obtained experimentally are demonstrated in Figure A1

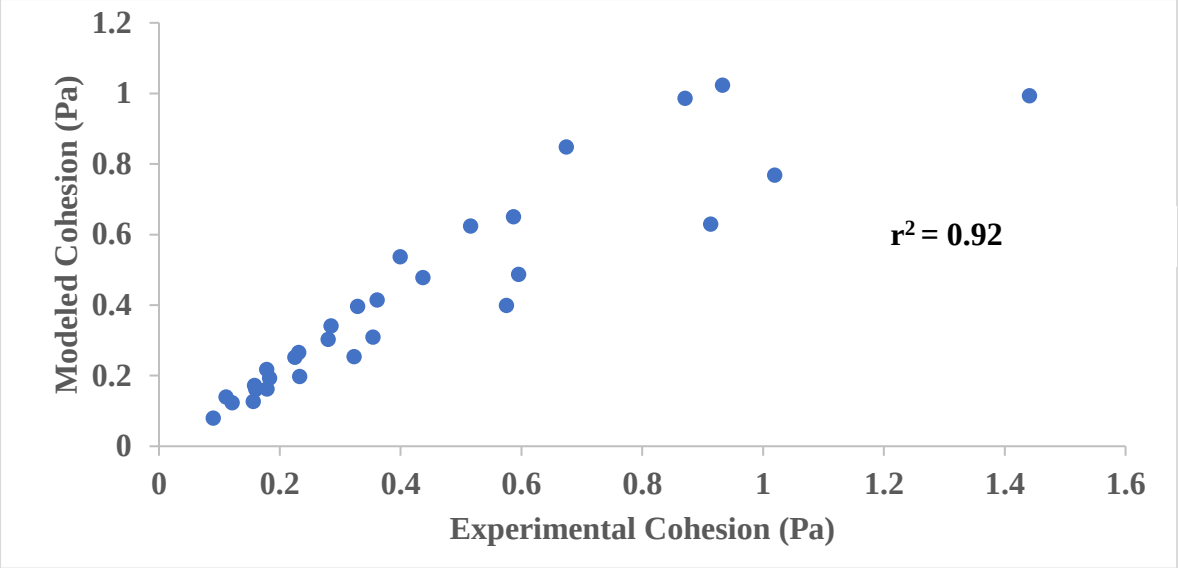

Figure A1: Comparison between experimental cohesion and modelled cohesion at all σ_{pre}

The above figure depicts, after performing regression analysis, there is 92% similarity in the values which were obtained through the model and the experimental data from the powder flow tester. The comparison of modeled σ_c values versus experimental σ_c values are demonstrated in Figure A2.

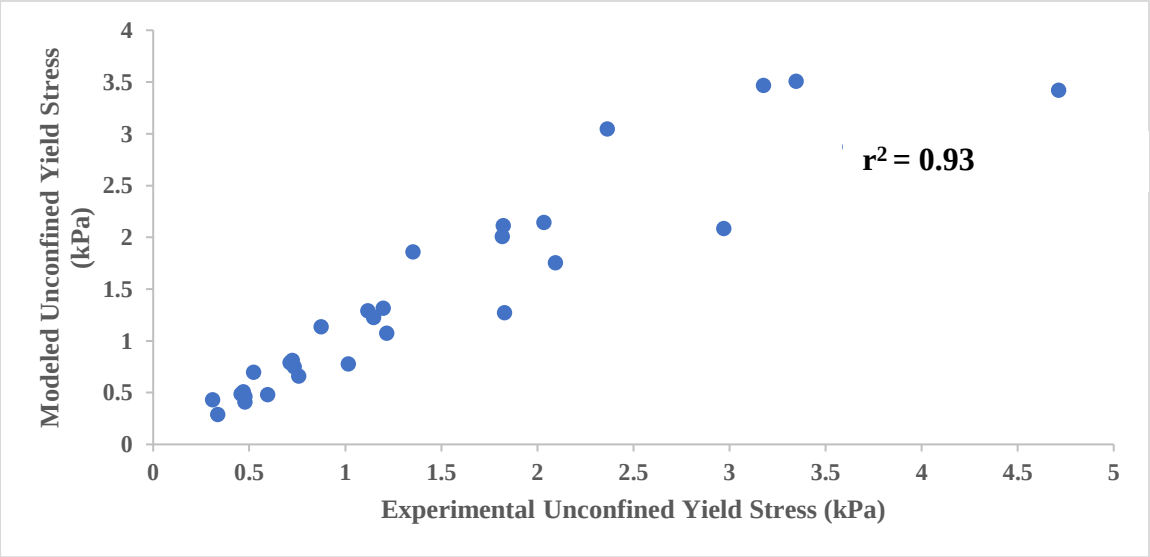

Figure A2. Comparison between experimental unconfined yield stress and modelled unconfined yield stress at all σ_{pre}

Later, for validation of the modeling method, the data of 25 samples of fly ash and cement were taken from Lokesh (2016) and the model of cohesion and unconfined yield stress is as given below:

$$C = 0.0653\ (d_{50}/S)^{1.171}(CI)^{-0.024}\left(\sigma_{pre}\right)^{0.692} \qquad [r^2 = 0.99]$$

$$\sigma_c = 0.0001\ (d_{50}/S)^{1.095}(CI)^{-0.017}\left(\sigma_{pre}\right)^{0.729} \qquad [r^2 = 0.99]$$

The comparison of the modeled cohesion values and the cohesion values obtained experimentally are demonstrated in Figure A3

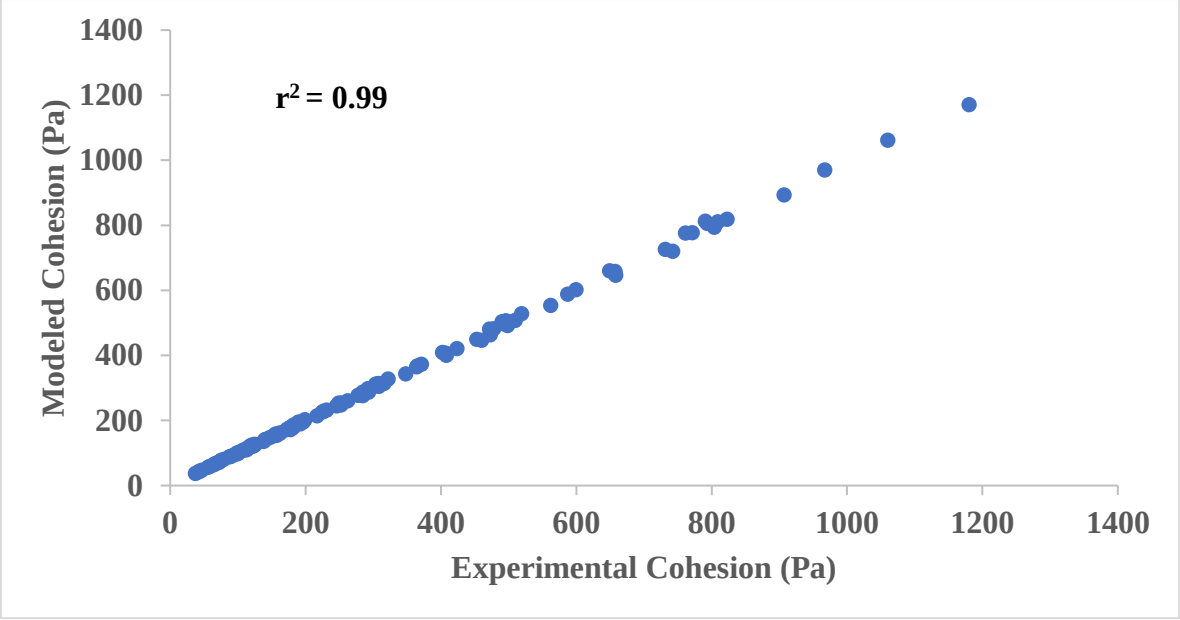

Figure A3. Comparison between experimental cohesion and modelled at all σ_{pre}

The above figure depicts, after performing regression analysis, there is 99% similarity in the values which were obtained through the model and the experimental data from the powder flow tester. The comparison of modeled σ_c values versus experimental σ_c values are demonstrated in Figure A4.

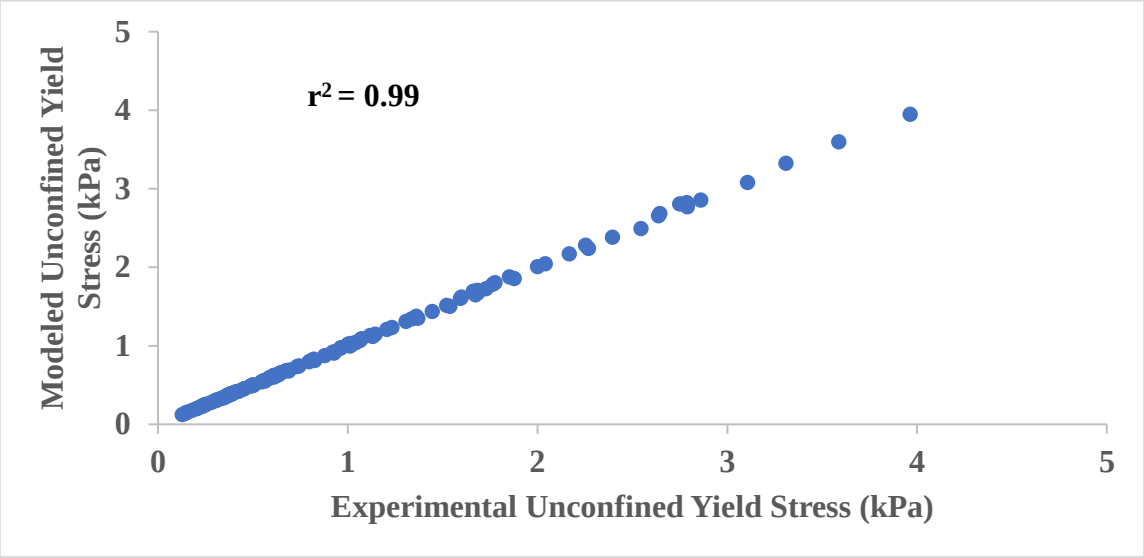

Figure A4. Comparison between experimental unconfined yield stress and modelled unconfined yield stress at all σ_{pre}

List of Publications

SCI Journal Publications

S.No	Title of the Paper	Author	SCI Journal	Impact Factor	Status
1	An Experimental Investigation into the Flow Properties of Lactose and Paracetamol Powders.	Garg, Vivek and Mallick, S.S.	Powder Technology, Elsevier	2.759	Under Review
2	An Experimental Investigation into the Flowability of Calcium Sulphate and Di-Calcium Phosphate Excipients used in Pharmaceutical Industries.	Garg, Vivek and Mallick, S.S.	European Journal of Pharmaceutical Sciences, Elsevier	3.773	Under Review
3	An Experimental Investigation into the Flow Properties of Starch and Magnesium Tri-Silicate used as Pharmaceutical Excipients.	Garg, Vivek and Mallick, S.S.	Powder Technology, Elsevier	2.759	Under Review
4	An Experimental Investigation into the Flowability of Detergents with the effect of Storage Condition.	Garg, Vivek and Mallick, S.S.	Journal of the Taiwan Institute of Chemical Engineers	2.848	Communicated
5	Modelling Flow Properties of Fine Dry Powders Using Particle Morphological Properties and its Effects on Geometry of Fly Ash Evacuation Hoppers	Mallick, S.S., Garg, Vivek, Rohilla, Lokesh and Setia, Gautam	Particulate Science and Technology	0.707	Under Review

Conference Publications

S.No	Title of the Paper	Author	Conference Name	Status
1	An Experimental Investigation into the Flow Properties of Pharmaceutical Powders	Garg, Vivek and Mallick, S.S.	RELPOWFLO V, Norway	Accepted